Investigating the Ability of PINNs To Solve Burgers' PDE Near Finite-Time BlowUp

Anonymous authors
Paper under double-blind review

Abstract

Physics Informed Neural Networks (PINNs) have been achieving ever newer feats of solving complicated PDEs numerically while offering an attractive trade-off between accuracy and speed of inference. A particularly challenging aspect of PDEs is that there exist simple PDEs which can evolve into singular solutions in finite time starting from smooth initial conditions. In recent times some striking experiments have suggested that PINNs might be good at even detecting such finite-time blow-ups. In this work, we embark on a program to investigate this stability of PINNs from a rigorous theoretical viewpoint. Firstly, we derive generalization bounds for PINNs for Burgers' PDE, in arbitrary dimensions, under conditions that allow for a finite-time blow-up. Then we demonstrate via experiments that our bounds are significantly correlated to the ℓ_2-distance of the neurally found surrogate from the true blow-up solution, when computed on sequences of PDEs that are getting increasingly close to a blow-up.

1 Introduction

Partial Differential Equations (PDEs) are used for modeling a large variety of physical processes from fluid dynamics to bacterial growth to quantum behaviour at the atomic scale. But differential equations that can be solved in “closed form,” that is, by means of a formula for the unknown function, are the exception rather than the rule. Hence over the course of history, many techniques for solving PDEs have been developed. However, even the biggest of industries still find it extremely expensive to implement the numerical PDE solvers – like airplane industries aiming to understand how wind turbulence pattern changes with changing aerofoil shapes, (Jameson et al., 2002) need to choose very fine discretizations which can often increase the run-times prohibitively.

In the recent past, deep learning has emerged as a competitive way to solve PDEs numerically. We note that the idea of using nets to solve PDEs dates back many decades Lagaris et al. (1998) (Broomhead & Lowe, 1988). In recent times this idea has gained significant momentum and “AI for Science” (Karniadakis et al., 2021) has emerged as a distinctive direction of research. Some of the methods at play for solving PDEs neurally (E et al., 2021) are the Physics Informed Neural Networks (PINNs) paradigm (Raissi et al., 2019) (Lawal et al., 2022), “Deep Ritz Method” (DRM, Yu et al. (2018)), “Deep Galerkin Method” (DGM, Sirignano & Spiliopoulos (2018)) and many further variations that have been developed of these ideas, (Kaiser et al., 2021; Erichson et al., 2019; Wandel et al., 2021; Li et al., 2022; Salvi et al., 2022). An overarching principle that many of these implement is to try to constrain the loss function by using the residual of the PDE to be solved.

These different data-driven methods of solving the PDEs can broadly be classified into two kinds, **(1)** ones which train a single neural net to solve a specific PDE and **(2)** operator methods – which train multiple nets in tandem to be able to solve a family of PDEs in one shot. (Fan et al., 2019; Lu et al., 2021; 2022; Wang et al., 2021b) The operator methods are particularly interesting when the underlying physics is not known and the state-of-the-art approaches of this type can be seen in works like Raonić et al. (2023), Kovachki et al. (2023) and Fan et al. (2019).

For this work, we focus on the PINN formalism from Raissi et al. (2019). Many studies have demonstrated the success of this setup in simulating complex dynamical systems like the Navier-Stokes PDE (Arthurs & King, 2021; Wang et al., 2020; Eivazi et al., 2022), the Euler PDE (Wang

Implementation is available at https://anonymized et al., 2022d), descriptions of shallow water wave by the Korteweg-De Vries PDEs (Hu et al., 2022a) and many more.

Work in Mishra & Molinaro (2022); De Ryck et al. (2022) has provided the first-of-its-kind bounds on the generalization error of PINNs for approximating various standard PDEs, including the Navier-Stokes' PDE. Such bounds strongly motivate why minimization of the PDE residual at collocation points can be a meaningful way to solve the corresponding PDEs. However, the findings and analysis in Krishnapriyan et al. (2021); Wang et al. (2021a) point out that the training dynamics of PINNs can be unstable and failure cases can be found among even simple PDE setups. It has also been studied that when trivial solutions can exist for the PDE, the PINN training can get stuck at those solutions Rohrhofer et al. (2022); Cheng Wong et al. (2022). Work in Wang et al. (2022b) has shown that traditional ways of solving PINNs can violate causality.

However, in all the test cases above the target solutions have always been nice functions. But an interesting possibility with various differential equations representing the time dynamics of some system is that their solution might have a finite-time blow-up. Blow-up is a phenomena where the solution becomes infinite at some points as t approaches a certain time $T < \infty$, while the solution is well-defined for all $0 < t < T$ i.e.

$$\sup_{x \in D} |\boldsymbol{u}(\boldsymbol{x}, t)| \to \infty \quad as \quad t \to T^-$$

One can see simple examples of this fascinating phenomenon, for example, for the following ODE $\frac{du}{dt} = u^2, \ u(0) = u_0, \ u_0 > 0$ it's easy to see that it's solution blows-up at $t = \frac{1}{u_0}$. Wintner's theorem (Wintner, 1945) provided a sufficient condition for a very generic class of ODEs for the existence of a well-defined solution for them over the entire time-domain, in other words, the non-existence of a finite-time blowup. More sophisticated versions of such sufficient conditions for global ODE solutions were subsequently developed Cooke (1955) and Pazy (1983) (Theorem 3.3). Non-existence of finite-time blow-ups have also been studied in control theory (Lin et al., 1996) under the name of "forward completeness" of a system.

The existence of a blow-up makes solving PDEs difficult to solve for classical approximation methods. There is a long-standing quest in numerical methods of PDE solving to be able to determine the occurrence, location and nature of finite time blow-ups (Stuart & Floater, 1990). A much investigated case of blow-up in PDE is for the exponential reaction model $\boldsymbol{u}_t = \Delta \boldsymbol{u} + \lambda e^{\boldsymbol{u}}, \quad \lambda > 0$ which was motivated as a model of combustion under the name Frank-Kamenetsky equation. The nature of blow-up here depends on the choice of λ, the initial data and the domain. Another such classical example is $\boldsymbol{u}_t = \Delta \boldsymbol{u} + \boldsymbol{u}^p$ and both these semi-linear equations were studied in the seminal works Fujita (1966; 1969) which pioneered systematic research into finite-time blow-ups of PDEs.

To the best of our knowledge, the behaviour PINNs in the proximity of finite-time blow-up has not received adequate attention in prior work on PINNs. We note that there are multiple real-world phenomena whose PDE models have finite-time blow-ups and these singularities are known to correspond to practically relevant processes – such as in chemotaxis models (Herrero & Velazquez, 1997; He & Tadmor, 2019; Chen et al., 2022; Tanaka, 2023) and thermal-runoff models (Bebernes & Kassoy, 1981; Lacey, 1983; Dold, 1991; Herrero & Velázquez, 1993; Lacey, 1995).

In light of the recent rise of methods for PDE solving by neural nets, it raises a curiosity whether the new methods, in particular PINNs, can be used to reliably solve PDEs near such blow-ups. While a general answer to this is outside the scope of this work, *we derive theoretical risk bounds for PINNs which are amenable to be tested against certain analytically describable finite-time blow-ups. Additionally, we give experiments to demonstrate that our bounds retain non-trivial insight even when tested in the proximity of such singularities.*

In Wang et al. (2022d), thought provoking experimental evidence was given that PINNs could potentially discover PDE solutions with blow-up even when their explicit descriptions are not known. Hence inspired, here we embark on a program to understand this interface from a rigorous viewpoint and show how well the theoretical risk bounds correlate to their experimentally observed values - in certain blow-up situations. As our focus point, we will use reduced models of fluid dynamics, i.e Burgers' PDE in one and two spatial dimensions. The choice of our test case is motivated by the fact that these PDE setups have analytic solutions with blow-up – as is necessary to do a controlled study of PINNs facing such a situation. We note that it is otherwise very rare to know exact fluid-like solutions which blow-up in finite-time (Tao, 2016a;b)

1.1 Informal Summary of Our Results

At the very outset, we note that to the best of our knowledge there are no available off-the-shelf generalization bounds for any setup of PDE solving by neural nets where the assumptions being made include any known analytic solution with blow-up for the corresponding PDE. So, as a primary step we derive new risk bounds for Burgers's PDE in Theorem 3.1 and Theorem 3.2, where viscosity is set to zero and its boundary conditions are consistent with finite-time blow-up cases of Burgers' PDE that we eventually want to test on. We note that despite being designed to cater to blow-up situations, the bound in Theorem 3.2 is also "stable" in the sense of Wang et al. (2022a).

Our experiments reveal that for our test case with Burgers' PDE while the theoretical error bounds we derive are vacuous (as is routine for neural net generalization bounds), somewhat surprisingly they do maintain a non-trivial amount of correlation with the L^2-distance of the derived solution from the true solution. The plot in Figures 1 and 5 vividly exhibit the presence of this strong correlation between the derived bounds and the true risk despite the experiments being progressively made on time domains such that the true solution is getting arbitrarily close to becoming singular.

A key feature of our approach to this investigation is that we do not tailor our theory to the experimental setups we test on later. We posit that this is a fair way to evaluate the reach of PINN theory whereby the theory is built such that it caters to any neural net and any solution of the PDE while these generically derived bounds get tested on the hard instances. [2]

1.2 A review of the framework of physics-informed neural networks

Consider the following specification of a PDE satisfied by an appropriately smooth function $\boldsymbol{u}(\boldsymbol{x},t)$

$$\begin{aligned} &\boldsymbol{u}_t + \mathcal{N}_{\boldsymbol{x}}[\boldsymbol{u}] = 0, \quad && \boldsymbol{x} \in D, t \in [0,T] \\ &\boldsymbol{u}(\boldsymbol{x},0) = h(\boldsymbol{x}), \quad && \boldsymbol{x} \in D \\ &\boldsymbol{u}(\boldsymbol{x},t) = g(\boldsymbol{x},t), \quad && \boldsymbol{t} \in [0,T], \boldsymbol{x} \in \partial D \end{aligned} \tag{1}$$

where $\boldsymbol{x}$ and t represent the space and time dimensions, subscripts denote the partial differentiation variables, $\mathcal{N}_{\boldsymbol{x}}[\boldsymbol{u}]$ is the nonlinear differential operator, D is a subset of $\mathbb{R}^d$ s.t it has a well-defined boundary ∂D. Following Raissi et al. (2019), we try to approximate $\boldsymbol{u}(\boldsymbol{x},t)$ by a deep neural network $\boldsymbol{u}_\theta(\boldsymbol{x},t)$, and then we can define the corresponding residuals as,

$$\mathcal{R}_{pde}(x,t) \coloneqq \partial_t \boldsymbol{u}_\theta + \mathcal{N}_{\boldsymbol{x}}[\boldsymbol{u}_\theta(\boldsymbol{x},t)],\ \mathcal{R}_t(x) \coloneqq \boldsymbol{u}_\theta(\boldsymbol{x},0) - h(\boldsymbol{x}),\ \mathcal{R}_b(x,t) \coloneqq \boldsymbol{u}_\theta(\boldsymbol{x},t) - g(\boldsymbol{x},t)$$

Note that the partial derivative of the neural network ($\boldsymbol{u}_\theta$) can be easily calculated using auto-differentiation (Baydin et al., 2018). The neural net is then trained on a loss function

$$\mathcal{L}(\theta) \coloneqq \mathcal{L}_{pde}(\theta) + \mathcal{L}_t(\theta) + \mathcal{L}_b(\theta)$$

where $\mathcal{L}_{pde}$, $\mathcal{L}_t$ and $\mathcal{L}_b$ penalize for $\mathcal{R}_{pde}$, $\mathcal{R}_t$ and $\mathcal{R}_b$ respectively for being non-zero. Typically it would take the form

$$\mathcal{L}_{pde} = \frac{1}{N_{pde}} \sum_{i=1}^{N_{pde}} \left|\mathcal{R}_{pde}(x_r^i, t_r^i)\right|^2,\ \mathcal{L}_t = \frac{1}{N_t} \sum_{i=1}^{N_t} \left|\mathcal{R}_t(x_t^i)\right|^2,\ \mathcal{L}_b = \frac{1}{N_b} \sum_{i=1}^{N_b} \left|\mathcal{R}_b(x_b^i, t_b^i)\right|^2$$

where (x_r^i, t_r^i) denotes the collocation points, (x_t^i) are the points sampled on the spatial domain for the initial loss and (x_b^i, t_b^i) are the points sampled on the boundary for the boundary loss. The aim here is to train a neural net $\boldsymbol{u}_\theta$ such that $\mathcal{L}_\theta$ is as close to zero as possible.

2 Related Works

To the best of our knowledge the most general population risk bound for PINNs has been proven in Hu et al. (2022b), and this result applies to all linear second order PDE and it is a Rademacher complexity based bound. This bound cannot be applied to our study since Burgers' PDE is not a linear PDE. Mishra & Molinaro (2022) derived generalization bounds for PINNs, that unlike Hu et al. (2022b), explicitly depend on the trained neural net. They performed the analysis for several

[2] One can surmise that it might be possible to build better theory exploiting information about the blow-ups - like if the temporal location of the blow-up is known. However, it is to be noted that building theory while assuming knowledge of the location of the blow-up might be deemed unrealistic given the real-world motivations for such phenomena.

PDEs, and the "viscous scalar conservation law" being one of them, which includes the $1 + 1$-Burgers' PDE. However for testing against analytic blow-up solutions, we need such bounds at zero viscosity unlike what is considered therein, and most critically, unlike Mishra & Molinaro (2022) we keep track of the prediction error at the spatial boundary of the computational domain with respect to non-trivial functional constraints.

De Ryck et al. (2022) derived a generalization bound for Navier-Stokes PDE, which too depends on the trained neural net. We note that, in contrast to the approach presented in De Ryck et al. (2022), our method does not rely on the assumption of periodicity in boundary conditions or divergence-lessness of the true solution. These flexibilities in our setup ensure that our bound applies to known analytic cases of finite-time blow-ups for the $d + 1$-Burgers' PDE.

Notwithstanding the increasing examples of the success of PINNs, it is known that PINNs can at times fail to converge to the correct solution even for basic PDEs – as reflected in several recent studies on characterizing the "failure modes" of PINNs. Studies by Wang et al. (2021a), and more recently by Daw et al. (2023) have demonstrated that sometimes this failure can be attributed to problems associated with the loss function, specifically the uneven distribution of gradients across various components of the PINN loss. Wang et al. (2021a) attempt to address this issue by assigning specific weights to certain parts of the loss function. While Daw et al. (2022) developed a way to preferentially sample collocation points with high loss and subsequently use them for training. Krishnapriyan et al. (2021) observed a similar issue within the structure of the loss function. While not changing the PINN loss function, they introduced two techniques: "curriculum regularization" and "sequence-to-sequence learning" for PINNs to enhance their performance. In Wang et al. (2022c) PINNs have been analyzed from a neural tangent kernel perspective to suggest that PINNs suffer from "spectral-bias"(Rahaman et al., 2019) which makes it more susceptible to failure in the presence of "high frequency features" in the target function. They propose a method for improving training by assigning weights to individual components of the loss functions, aiming to mitigate the uneven convergence rates among the various loss elements.

Notation In the subsequent section we use $d + 1$ to represent dimensions, here d is the number of spatial dimensions and 1 is always the temporal dimension. Nabla (∇) is used to represent the differential operator i.e. $(\frac{\partial}{\partial x_1}, \ldots, \frac{\partial}{\partial x_d})$. And for any real function u on a domain D, $\|u(x)\|_{L^\infty(D)}$ will represent $\sup_{x \in D} |u(x)|$.

3 Main Results

3.1 Generalization Bounds for the $(d + 1)$-dimensional Burgers' PDE

The PDE that we consider is as follows,

$$\begin{aligned} \partial_t \boldsymbol{u} + (\boldsymbol{u} \cdot \nabla)\boldsymbol{u} &= 0 \\ \boldsymbol{u}(t = t_0) &= \boldsymbol{u}_{t_0} \end{aligned} \tag{2}$$

Here $\boldsymbol{u} : D \times [t_0, T] \to \mathbb{R}^d$ is the fluid velocity and $\boldsymbol{u}_{t_0} : D \to \mathbb{R}^d$ is the initial velocity. Then corresponding to a surrogate solution $\boldsymbol{u}_\theta$ we define the residuals as,

$$\mathcal{R}_{\text{pde}} \coloneqq \partial_t \boldsymbol{u}_\theta + (\boldsymbol{u}_\theta \cdot \nabla)\boldsymbol{u}_\theta \tag{3}$$

$$\mathcal{R}_{\text{t}} \coloneqq \boldsymbol{u}_\theta(t = t_0) - \boldsymbol{u}(t = t_0) \tag{4}$$

Corresponding to the true solution $\boldsymbol{u}$, we will define the L^2- risk of any surrogate solution $\boldsymbol{u}_\theta$ as,

$$\int_\Omega \|\boldsymbol{u}(\boldsymbol{x}, t) - \boldsymbol{u}_\theta(\boldsymbol{x}, t)\|_2^2 \, \mathrm{d}\boldsymbol{x} \, \mathrm{d}t$$

In the following theorem we consider $t_0 = \frac{-1}{\sqrt{2}} + \delta$ and $T = \delta$ for some $\delta > 0$. Here the spatial domain is represented by $D \subset \mathbb{R}^d$ and Ω represents the whole domain $D \times [t_0, T]$.

Theorem 3.1. *Let $d \in \mathbb{N}$ and $\boldsymbol{u} \in C^1(D \times [t_0, T])$ be the unique solution of the (d+1)-dimensional Burgers' equation given in equation 2. Then for any C^1 surrogate solution to equation 2, say $\boldsymbol{u}_\theta$, the L^2-risk with respect to the true solution is bounded as,*

$$\log\left(\int_\Omega \|\boldsymbol{u}(\boldsymbol{x}, t) - \boldsymbol{u}_\theta(\boldsymbol{x}, t)\|_2^2 \, \mathrm{d}\boldsymbol{x} \, \mathrm{d}t\right) \le \log\left(\frac{C_1 C_2}{4}\right) + \frac{C_1}{\sqrt{2}} \tag{5}$$

where,

$$\begin{aligned}C_1 &= d^2 \|\nabla \boldsymbol{u}_\theta\|_{L^\infty(\Omega)} \\ &\quad + 1 + d^2 \|\nabla \boldsymbol{u}\|_{L^\infty(\Omega)} \\ C_2 &= \int_D \|\mathcal{R}_t\|_2^2 \,\mathrm{d}\boldsymbol{x} + \int_\Omega \|\mathcal{R}_{pde}\|_2^2 \,\mathrm{d}\boldsymbol{x}\,\mathrm{d}t + d^2 \|\nabla \boldsymbol{u}_\theta\|_{L^\infty(\Omega)} \int_\Omega \|\boldsymbol{u}_\theta\|_2^2 \,\mathrm{d}\boldsymbol{x}\,\mathrm{d}t \\ &\quad + d^2 \|\nabla \boldsymbol{u}\|_{L^\infty(\Omega)} \int_\Omega \|\boldsymbol{u}\|_2^2 \,\mathrm{d}\boldsymbol{x}\,\mathrm{d}t\end{aligned}$$

The theorem above has been proved in Appendix A.1 We note that the bound presented in equation 5 does not make any assumptions about the existence of a blow-up in the solution and its applicable to all solutions that have continuous first derivatives however large, as would be true for the situations very close to blow-up as we would consider. Also, we note that the bound in De Ryck et al. (2022) makes assumptions (as was reviewed in Section 2) which (even if set to zero pressure) prevent it from being directly applicable to the setup above which can capture analytic solutions arbitrarily close to finite-time blow-up.

Secondly, note that these bounds are not dependent on the details of the loss function that might eventually be used in the training to obtained the $\boldsymbol{u}_\theta$. In that sense such a bound is more universal than usual generalization bounds which depend on the loss.

Lastly, note that the inequality proven in Theorem 3.1 bounds the distance of the true solution from a PINN solution in terms of (a) norms of the true solution and (b) various integrals of the found solution like its norms and unsupervised risks on the computation domain. Hence this is not like usual generalization bounds that get proven in deep-learning theory literature where the LHS is the population risk and RHS is upperbounding that by a function that is entirely computable from knowing the training data and the trained net. Being in the setup of solving PDEs via nets lets us contruct such new kinds of bounds which can exploit knowledge of the true PDE solution.

While Theorem 3.1 is applicable to Burgers' equations in any dimensions, it becomes computationally very expensive to compute the bound in higher dimensions. Therefore, in order to better our intuitive understanding, we separately analyze the case of $d = 1$, in the upcoming Section 3.2. Furthermore, the RHS of (5) only sees the errors at the initial time and in the space-time bulk. In general dimensions it is rather complicated to demonstrate that being able to measure the boundary risks of the surrogate solution can be leveraged to get stronger generalization bounds. But this can be transparently kept track of in the $d = 1$ case - as we will demonstrate now for a specific case with finite-time blow-up. Along the way, it will also be demonstrated that the bounds possible in one dimension - are "stable" in a precise sense as will be explained after the following theorem.

3.2 Generalization Bounds for a Finite-Time Blow-Up Scenario with (1+1)-dimensional Burgers' PDE

For $u : [-1, 1] \times [t_0, T] \to \mathbb{R}$ being at least once continuously differentiable in each of its variables we consider a Burgers's PDE as follows on the space domain being $[-1, 1]$ and the two limits of the time domain being specified as $t_0 = -1 + \delta$ and $T = \delta$ for any $\delta > 0$,

$$\begin{aligned}u_t + u u_x &= 0 \\ u(x, -1 + \delta) &= \frac{x}{-2 + \delta} \\ u(-1, t) = \frac{1}{1 - t} \ &; \ u(1, t) = \frac{1}{t - 1}\end{aligned} \tag{6}$$

We note that in the setup for Burger's PDE being solved by neural nets that was analyzed in the pioneering work in Mishra & Molinaro (2022), the same amount of information was assumed to be known i.e the PDE, an initial condition and boundary conditions at the spatial boundaries. However in here, the values we choose for the above constraints are non-trivial and designed to cater to a known solution for this PDE i.e $u = \frac{x}{t-1}$ which blows up at $t = 1$.

For any C^1 surrogate solution to the above, say u_θ its residuals can be written as,

$$\mathcal{R}_{int,\theta}(x,t) \coloneqq \partial_t(u_\theta(x,t)) + \partial_x \frac{u_\theta^2(x,t)}{2} \tag{7}$$

$$\mathcal{R}_{tb,\theta}(x) \coloneqq u_\theta(x,-1+\delta) - \frac{x}{-2+\delta} \tag{8}$$

$$(\mathcal{R}_{sb,-1,\theta}(t), \mathcal{R}_{sb,1,\theta}(t)) \coloneqq \left(u_\theta(-1,t) - \frac{1}{1-t},\ u_\theta(1,t) - \frac{1}{t-1}\right) \tag{9}$$

We define the L^2−risk of u_θ with respect to the true solution u of equation 6 as,

$$\mathcal{E}_G(u_\theta) \coloneqq \left(\int_{-1+\delta}^{\delta}\int_{-1}^{1} |u(x,t) - u_\theta(x,t)|^2 \, dxdt\right)^{\frac{1}{2}} \tag{10}$$

Theorem 3.2. *Let $u \in C^k((-1+\delta,\delta)\times(-1,1))$ be the unique solution of the one dimensional Burgers' PDE in equation 6, for any $k \geq 1$. Then for any surrogate solution for the same PDE, say $u^* \coloneqq u_{\theta^*}$ its risk as defined in equation 10 is bounded as,*

$$\begin{aligned}\mathcal{E}_G^2 \leq \left[1 + Ce^C\right] \Bigg[&\int_{-1}^{1} \mathcal{R}_{tb,\theta^*}(x)dx + 2C_{2b}\left(\int_{-1+\delta}^{\delta} \mathcal{R}^2_{sb,-1,\theta^*}(t)dt + \int_{-1+\delta}^{\delta} \mathcal{R}^2_{sb,1,\theta^*}(t)dt\right) \\ &+ 2C_{1b}\left(\left(\int_{-1+\delta}^{\delta} \mathcal{R}^2_{sb,-1,\theta^*}(t)dt\right)^{\frac{1}{2}} + \left(\int_{-1+\delta}^{\delta} \mathcal{R}^2_{sb,1,\theta^*}(t)dt\right)^{\frac{1}{2}}\right) \\ &+ \int_{-1+\delta}^{\delta}\int_{-1}^{1} \mathcal{R}^2_{int,\theta^*}(x,t)dxdt\Bigg]\end{aligned} \tag{11}$$

where $C = 1 + 2C_{u_x}$, with $C_{u_x} = \|u_x\|_{L^\infty((-1+\delta,\delta)\times(-1,1))} = \left\|\frac{1}{t-1}\right\|_{L^\infty([-1+\delta,\delta])} = \frac{1}{1-\delta}$ and

$$\begin{aligned} C_{1b} &= \|u(1,t)\|^2_{L^\infty([-1+\delta,\delta])} = \left\|\frac{1}{1-t}\right\|^2_{L^\infty([-1+\delta,\delta])} = \frac{1}{(1-\delta)^2} \\ C_{2b} &= \|u_{\theta^*}(1,t)\|_{L^\infty([-1+\delta,\delta])} + \frac{3}{2}\left\|\frac{1}{t-1}\right\|_{L^\infty([-1+\delta,\delta])} = \|u_{\theta^*}(1,t)\|_{L^\infty([-1+\delta,\delta])} + \frac{3}{2}\left(\frac{1}{1-\delta}\right) \end{aligned} \tag{12}$$

The theorem above has been proved in Appendix A.3. Note that the RHS of equation 11 is evaluatable without exactly knowing the eact true solution – the constants in equation 11 only requires some knowledge of the supremum value of u at the spatial boundaries and the behaviour of the first order partial derivative of u.

Most importantly, Theorem 3.2 shows that despite the setting here being of proximity to finite-time blow-up, the naturally motivated PINN risk in this case [3] is "(L_2, L_2, L_2, L_2)-stable"[4] in the precise sense as defined in Wang et al. (2022a). This stability property being true implies that if the PINN risk of the solution obtained is measured to be $\mathcal{O}(\epsilon)$ then it would directly imply that the L_2-risk with respect to the true solution (10) is also $\mathcal{O}(\epsilon)$. And this would be determinable *without having to know the true solution at test time.*

In Appendix A.4 we apply quadrature rules on (11) and show a version of the above bound which makes the sample size dependency of the bound more explicit.

4 Experiments

Our experiments are designed to demonstrate the efficacy of the generalization error bounds discussed in Section 3 in the vicinity of finite-time blow-ups happening in our use cases. Towards motivating the novelty of our setup we give a brief overview of how demonstrations of deep-learning generalization bounds have been done in the recent past.

[3] PINN risk is defined as $\mathbb{E}[|\mathcal{R}_{int,\theta}(x,t)|^2] + \mathbb{E}[|\mathcal{R}_{tb,\theta}|^2] + \mathbb{E}[|\mathcal{R}_{sb,-1,\theta}|^2] + \mathbb{E}[|\mathcal{R}_{sb,1,\theta}|^2]$

[4] Suppose Z_1, Z_2, Z_3, Z_4 are four Banach spaces, a PDE defined by (1) is Z_1, Z_2, Z_3, Z_4-stable, if $\|\boldsymbol{u}_\theta(x,t) - \boldsymbol{u}(x,t)\|_{Z4} = \mathcal{O}(\|\partial_t \boldsymbol{u}_\theta + \mathcal{N}_{\boldsymbol{x}}[\boldsymbol{u}_\theta(\boldsymbol{x},t)]\|_{Z_1} + \|\boldsymbol{u}_\theta(\boldsymbol{x},0) - h(\boldsymbol{x})\|_{Z_2} + \|\boldsymbol{u}_\theta(\boldsymbol{x},t) - g(\boldsymbol{x},t)\|_{Z_3})$ as $\|\partial_t \boldsymbol{u}_\theta + \mathcal{N}_{\boldsymbol{x}}[\boldsymbol{u}_\theta(\boldsymbol{x},t)]\|_{Z_1}, \|\boldsymbol{u}_\theta(\boldsymbol{x},0) - h(\boldsymbol{x})\|_{Z_2}, \|\boldsymbol{u}_\theta(\boldsymbol{x},t) - g(\boldsymbol{x},t)\|_{Z_3} \to 0$ for any $\boldsymbol{u}_\theta$

In the thought-provoking paper Dziugaite & Roy (2017) the authors had computed their bounds for 2-layer neural nets at various widths to show the non-vacuous nature of their bounds. But these bounds are not applicable to any single neural net but to an expected neural net sampled from a specified distribution. Inspired by these experiments, works like Neyshabur et al. (2017) and Mukherjee (2020) perform a de-randomized PAC-Bayes analysis on the generalization error of neural nets - which can be evaluated on any given net.

In works such as Neyshabur et al. (2018) we see a bound based on Rademacher analysis of the generalization error and the experiments were performed for depth-2 nets at different widths to show the decreasing nature of their bound with increasing width – a very rare property to be true for uniform convergence based bounds. It is important to point out that the training data is kept fixed while changing the width of the neural net in Dziugaite & Roy (2017) and Neyshabur et al. (2018).

In Arora et al. (2018) the authors instantiated a way to do compression of nets and computed the bounds on a compressed version of the original net. More recently in Muthukumar & Sulam (2023) the authors incorporated the sparsity of a neural net alongside the PAC-Bayed analysis to get a better bound for the generalization error. In their experiments, they vary the data size while keeping the neural net fixed and fortuitously the bound becomes non-vacuous for a certain width of the net.

In this work, we investigate if theory can capture the performance of PINNs near a finite-time blow-up and if larger neural nets can better capture the nature of generalization error close to the blow-up. To this end, in contrast to the previous literature cited above, we keep the neural net fixed and vary the domain of the PDE. More specifically, progressively we choose time-domains arbitrarily close to the finite-time blow-up and test the theory at that difficult edge.

4.1 The Finite-Time Blow-Up Case of (1+1)-dimensional Burgers PDE from Section 3.2

The neural networks we use here have a depth of 6 layers, and we experiment at two distinct uniform widths of 30 and 300 neurons. For training, we use full-batch Adam optimizer for $100,000$ iterations and a learning rate of 10^{-4}. We subsequently select the model with the lowest training error for further analysis. In Figures 1a and 1b we see that the LHS and the RHS of equation 11 measured on the trained models is such that the correlation is very high (~ 1) over multiple values of the proximity parameter – up to being very close to the blow-up point. We also note that the correlation increases with the width of the neural net, a desirable phenomenon that our bound does capture – albeit implicitly. In Figure 3 in the appendix, we illustrate that the upper-bound derived in Theorem 3.2 does indeed fall over a reasonable range of widths at a fixed δ. The mean and the standard deviations plotted therein are obtained over six iterations of the experiment at different random seeds.

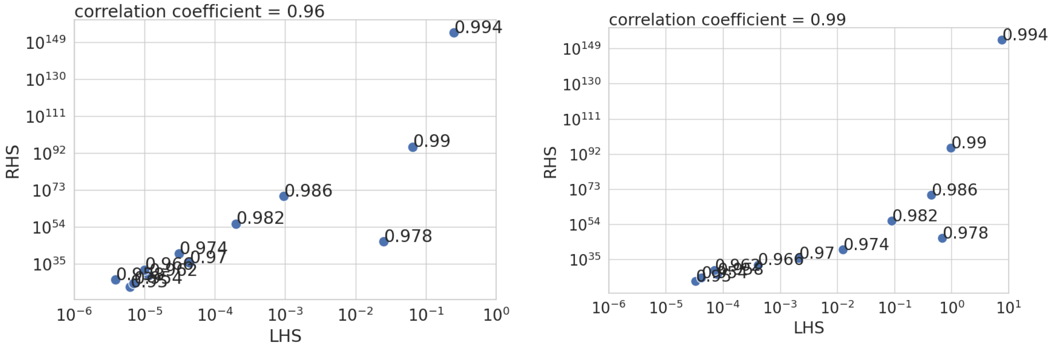

(a) width=30

(b) width=300

Figure 1: Demonstration of the presence of high correlation between the LHS (the true risk) and the RHS (and the derived bound) of equation (11) in Theorem 3.2 over PDE setups increasingly close to the singularity. Each experiment is labeled with the value of δ in the setup of equation 6 that it corresponds to.

4.2 Testing Against a (2+1)-dimensional Exact Burgers' Solution with Finite-Time Blow-Up

From (Biazar & Aminikhah, 2009) we know that there is an exact finite-time blow-up solution for Burgers' PDE in equation 2 for the case of $d = 2$,

$$u_1 = \frac{x_1 + x_2 - 2x_1 t}{1 - 2t^2},\ u_2 = \frac{x_1 - x_2 - 2x_2 t}{1 - 2t^2}$$

where u_i denotes the i^{th} component of the velocity being solved for. Note that at $t = 0$, both the above velocities are smooth while they eventually develop singularities at $t = \frac{1}{\sqrt{2}}$ - as is the expected hallmark of non-trivial finite-time blow-up solutions of PDEs. Also note that this singularity is more difficult to solve for since it is blowing up as $\mathcal{O}(\frac{1}{t^2})$ as compared to the $\mathcal{O}(\frac{1}{t})$ blow-up in the previous section in one dimension.

We set ourselves to the task of solving for this on a sequence of computational domains $x_1, x_2 \in [0, 1]$ and $t \in [-\frac{1}{\sqrt{2}} + \delta, \delta]$ where $\delta \in [0, \frac{1}{\sqrt{2}})$. Hence we have a sequence of PDEs to solve for – parameterized by δ and larger δs getting close to the blow-up. Let $g_{x_1,0}(x_2, t)$ and $g_{x_1,1}(x_2, t)$ be the boundary conditions for u_1 at $x_1 = 0$ & 1. Let $g_{x_2,0}(x_1, t)$ and $g_{x_2,1}(x_1, t)$ be the boundary conditions for u_2 at $x_2 = 0$ & 1 and u_{1,t_0} and u_{2,t_0} with $t_0 = -\frac{1}{\sqrt{2}} + \delta$ be the initial conditions for the two components of the velocity field. Hence the PDE we seek to solve is,

$$\left\{\ \boldsymbol{u}_t + (\boldsymbol{u} \cdot \nabla)\boldsymbol{u} = 0\right. \quad , \left\{\begin{array}{l} u_{1,t_0} = \frac{(1+\sqrt{2}-2\delta)x_1 + x_2}{2\delta(\sqrt{2}-\delta)} \\ u_{2,t_0} = \frac{x_1 - (1-\sqrt{2}+2\delta)x_2}{2\delta(\sqrt{2}-\delta)} \end{array}\right. , \left\{\begin{array}{l} g_{x_1,0}(x_2,t) \coloneqq u_1(x_1 = 0) = \frac{x_2}{1-2\cdot t^2} \\ g_{x_1,1}(x_2,t) \coloneqq u_1(x_1 = 1) = \frac{1+x_2-2\cdot t}{1-2\cdot t^2} \\ g_{x_2,0}(x_1,t) \coloneqq u_2(x_2 = 0) = \frac{x_1}{1-2\cdot t^2} \\ g_{x_2,1}(x_1,t) \coloneqq u_2(x_2 = 1) = \frac{x_1-1-2\cdot t}{1-2\cdot t^2} \end{array}\right. \tag{13}$$

Let $\mathcal{N} : \mathbb{R}^3 \to \mathbb{R}^2$ be the neural net to be trained, with output coordinates labeled as $(\mathcal{N}_{u_1}, \mathcal{N}_{u_2})$. Using this net we define the neural surrogates for solving the above PDE as,

$$u_{1,\theta} \coloneqq \mathcal{N}_{u_1}(x_1, x_2, t) \ \ u_{2,\theta} \coloneqq \mathcal{N}_{u_2}(x_1, x_2, t)$$

Correspondingly we define the PDE population risk, $\mathcal{R}_{pde}$ as,

$$\mathcal{R}_{pde} = \|\partial_t \boldsymbol{u}_\theta + \boldsymbol{u}_\theta \cdot \nabla \boldsymbol{u}_\theta\|^2_{[0,1]^2 \times [-\frac{1}{\sqrt{2}}+\delta,\delta],\nu_1} \tag{14}$$

In the above $\boldsymbol{u}_\theta = (u_{1,\theta}, u_{2,\theta})$ and ν_1 is a measure on the whose space-time domain $[0, 1]^2 \times [-\frac{1}{\sqrt{2}} + \delta, \delta]$. Corresponding to a measure ν_2 on $[0, 1] \times [-\frac{1}{\sqrt{2}} + \delta, \delta]$ (first interval being space and the later being time), we define $\mathcal{R}_{s,0}$ and $\mathcal{R}_{s,1}$ corresponding to violation of the boundary conditions,

$$\begin{aligned} \mathcal{R}_{s,0} &= \|u_{1,\theta} - g_{x_1,0}(x_2,t)\|^2_{\{0\}\times[0,1]\times[-\frac{1}{\sqrt{2}}+\delta,\delta],\nu_2} + \|u_{2,\theta} - g_{x_2,0}(x_1,t)\|^2_{[0,1]\times\{0\}\times[-\frac{1}{\sqrt{2}}+\delta,\delta],\nu_2} \\ \mathcal{R}_{s,1} &= \|u_{1,\theta} - g_{x_1,1}(x_2,t)\|^2_{\{1\}\times[0,1]\times[-\frac{1}{\sqrt{2}}+\delta,\delta],\nu_2} + \|u_{2,\theta} - g_{x_2,1}(x_1,t)\|^2_{[0,1]\times\{1\}\times[-\frac{1}{\sqrt{2}}+\delta,\delta],\nu_2} \end{aligned} \tag{15}$$

For a choice of measure ν_3 on the spatial volume $[0, 1]^2$ we define $\mathcal{R}_t$ corresponding to the violation of initial conditions $\boldsymbol{u}_{t_0} = (u_1(t_0), u_2(t_0))$,

$$\mathcal{R}_t = \|\boldsymbol{u}_\theta - \boldsymbol{u}_{t_0}\|^2_{[0,1]^2, t=t_0, \nu_3} \tag{16}$$

Thus the population risk we are looking to minimize is, $\mathcal{R} = \mathcal{R}_{pde} + \mathcal{R}_{s,0} + \mathcal{R}_{s,1} + \mathcal{R}_t$

We note that for the exact solution given above the constants in Theorem 3.1 evaluate to,

$$\begin{aligned} C_1 &= 2^2 \|\nabla \boldsymbol{u}_\theta\|_{L^\infty(\Omega)} \\ &\quad + 1 + 2^2 \max_{t=\frac{1}{\sqrt{2}}+\delta,\delta} \left\{ \left|\frac{1-2t}{1-2t^2}\right| + \left|\frac{1}{1-2t^2}\right|, \left|\frac{1}{1-2t^2}\right| + \left|\frac{1+2t}{1-2t^2}\right| \right\} \\ C_2 &= \int_D \|\mathcal{R}_t\|_2^2 \,\mathrm{d}\boldsymbol{x} + \int_{\tilde{\Omega}} \|\mathcal{R}_{pde}\|_2^2 \,\mathrm{d}\boldsymbol{x}\,\mathrm{d}t + 2^2 \|\nabla \boldsymbol{u}_\theta\|_{L^\infty(\Omega)} \int_{\tilde{\Omega}} \|\boldsymbol{u}_\theta\|_2^2 \,\mathrm{d}\boldsymbol{x}\,\mathrm{d}t \\ &\quad + 2^2 \max_{t=\frac{1}{\sqrt{2}}+\delta,\delta} \left\{ \left|\frac{1-2t}{1-2t^2}\right| + \left|\frac{1}{1-2t^2}\right|, \left|\frac{1}{1-2t^2}\right| + \left|\frac{1+2t}{1-2t^2}\right| \right\} \int_{\tilde{\Omega}} \|\boldsymbol{u}\|_2^2 \,\mathrm{d}\boldsymbol{x}\,\mathrm{d}t \end{aligned}$$

$$= \int_D \|\mathcal{R}_t\|_2^2 \, \mathrm{d}\boldsymbol{x} + \int_{\tilde{\Omega}} \|\mathcal{R}_{pde}\|_2^2 \, \mathrm{d}\boldsymbol{x} \, \mathrm{d}t + 2^2 \|\nabla \boldsymbol{u}_\theta\|_{L^\infty(\Omega)} \int_{\tilde{\Omega}} \|\boldsymbol{u}_\theta\|_2^2 \, \mathrm{d}\boldsymbol{x} \, \mathrm{d}t$$

$$+ 2^2 \max_{t=\frac{1}{\sqrt{2}}+\delta,\delta} \left\{ \left| \frac{1-2t}{1-2t^2} \right| + \left| \frac{1}{1-2t^2} \right|, \left| \frac{1}{1-2t^2} \right| + \left| \frac{1+2t}{1-2t^2} \right| \right\} \left[\frac{11t-7}{12(1-2t^2)} + \frac{5t+1}{12(1-2t^2)} \right]_{t=\frac{1}{\sqrt{2}}+\delta}^{\delta}$$

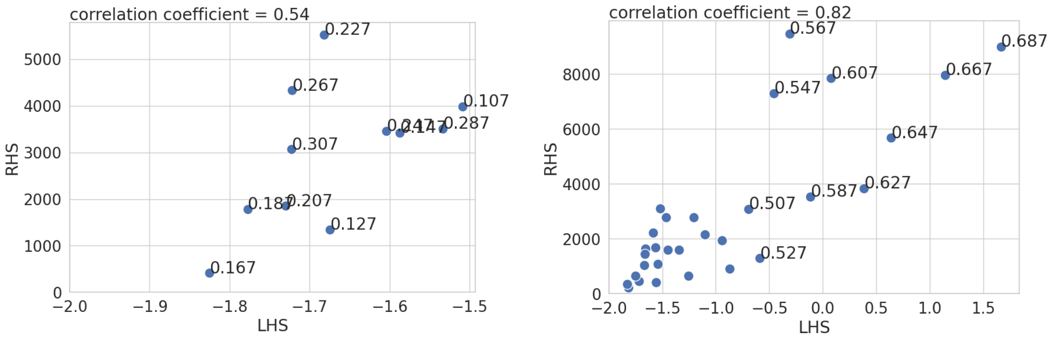

(a) width=30

(b) width=100

Figure 2: These plots show the behaviour of LHS (the true risk) and RHS (the derived bound) of equation (5) in Theorem 3.1 for different values of the δ parameter that quantifies proximity to the blow-up point. In the left plot each point is marked with the value of the δ at which the experiment is done and the right figure, for clarity, this is marked only for experiments at $\delta > \frac{1}{2}$.

In figure 5 we see the true risk and the derived bound in Theorem 3.1 for depth 6 neural nets obtained by training on the above loss. The experiments show that the insight from the previous demonstration continues to hold and more vividly so. Here, for the experiments at low width (30) the correlation stays around 0.50 until only $\delta = 0.307$, and beyond that it decreases rapidly. However, for experiments at width 100 the correlation remains close to 0.80 for δ much closer to the blow-up i.e at $\frac{1}{\sqrt{2}}$.

5 Concluding Discussions

In this work we have taken some of the first-of-its kind steps to initiate research into understanding the ability of neural nets to solve PDEs at the edge of finite-time blow-up. Our work suggests a number of exciting directions of future research. Firstly, more sophisticated modifications to the PINN formalism could be found to solve PDEs specifically near finite-time blow-ups.

Secondly, we note that it remains an open question to establish if there is any PINN risk for the $d+1$-dimensional Burgers, for $d > 1$, that is stable by the condition stated in Wang et al. (2022a), as was shown to be true in our $1+1$-dimensional Burgers in Theorem 3.2.

In Luo & Hou (2014b) the authors had given numerical studies to suggest that 3D incompressible Euler PDEs can develop finite-time singularities from smooth initial conditions for the fluid velocity. For their setup of axisymmetric fluid flow they conjectured a simplified model for the resultant flow near the outer boundary of the cylinder. Self-similar finite-time blow-ups for this model's solutions were rigorously established in Chen et al. (2022) - and it was shown that an estimate of its blowup-exponent is very close to the measured values of the 3D Euler PDE. In the seminal paper Elgindi (2021) it was shown that the unique local solution to 3D incompressible Euler PDEs can develop finite-time singularities despite starting from a divergence-free and odd initial velocity in $\mathbb{C}^{1,\alpha}$ and initial vorticity bounded as $\sim \frac{1}{1+\|x\|^\alpha}$. This breakthrough was built upon to prove the existence of finite time singularity in 2D Boussinesq PDE in Chen & Hou (2021).

Luo & Hou (2014a) highlighted the association between blow-ups in 3D Euler and 2D Boussinesq PDEs. In Wang et al. (2022d), the authors investigated the ability for PINNs to detect the occurrence of self-similar blow-ups in 2D Boussinesq PDE. A critical feature of this experiment was its use of the unconventional regularizer on the gradients of the neural surrogate with respect to its inputs. In light of this, we posit that a very interesting direction of research would be to investigate if a theoretical analysis of the risk bound for such losses can be used as a method of detection of the blow-up.

References

Sanjeev Arora, Rong Ge, Behnam Neyshabur, and Yi Zhang. Stronger generalization bounds for deep nets via a compression approach. In Jennifer Dy and Andreas Krause (eds.), *Proceedings of the 35th International Conference on Machine Learning*, volume 80 of *Proceedings of Machine Learning Research*, pp. 254–263. PMLR, 10–15 Jul 2018. URL https://proceedings.mlr.press/v80/arora18b.html.

Christopher J. Arthurs and Andrew P. King. Active training of physics-informed neural networks to aggregate and interpolate parametric solutions to the navier-stokes equations. *Journal of Computational Physics*, 438:110364, 2021. ISSN 0021-9991. doi: https://doi.org/10.1016/j.jcp.2021.110364. URL https://www.sciencedirect.com/science/article/pii/S002199912100259X.

Atilim Gunes Baydin, Barak A Pearlmutter, Alexey Andreyevich Radul, and Jeffrey Mark Siskind. Automatic differentiation in machine learning: a survey. *Journal of Marchine Learning Research*, 18:1–43, 2018.

JW Bebernes and DR Kassoy. A mathematical analysis of blowup for thermal reactions—the spatially nonhomogeneous case. *SIAM Journal on Applied Mathematics*, 40(3):476–484, 1981.

Jafar Biazar and Hossein Aminikhah. Exact and numerical solutions for non-linear burger's equation by vim. *Mathematical and Computer Modelling*, 49(7-8):1394–1400, 2009.

David Broomhead and David Lowe. Radial basis functions, multi-variable functional interpolation and adaptive networks. *ROYAL SIGNALS AND RADAR ESTABLISHMENT MALVERN (UNITED KINGDOM)*, RSRE-MEMO-4148, 03 1988.

Jiajie Chen and Thomas Y Hou. Finite time blowup of 2d boussinesq and 3d euler equations with c^ 1, α c 1, α velocity and boundary. *Communications in Mathematical Physics*, 383:1559–1667, 2021.

Jiajie Chen, Thomas Y Hou, and De Huang. Asymptotically self-similar blowup of the hou-luo model for the 3d euler equations. *Annals of PDE*, 8(2):24, 2022.

Jian Cheng Wong, Chinchun Ooi, Abhishek Gupta, and Yew-Soon Ong. Learning in sinusoidal spaces with physics-informed neural networks. *IEEE Transactions on Artificial Intelligence*, pp. 1–15, 2022. doi: 10.1109/TAI.2022.3192362.

K. L. Cooke. A non-local existence theorem for systems of ordinary differential equations. *Rendiconti del Circolo Matematico di Palermo*, 4(3):301–308, Sep 1955. ISSN 1973-4409. doi: 10.1007/BF02854201. URL https://doi.org/10.1007/BF02854201.

Arka Daw, Jie Bu, Sifan Wang, Paris Perdikaris, and Anuj Karpatne. Rethinking the importance of sampling in physics-informed neural networks. *arXiv preprint arXiv:2207.02338*, 2022.

Arka Daw, Jie Bu, Sifan Wang, Paris Perdikaris, and Anuj Karpatne. Mitigating propagation failures in physics-informed neural networks using retain-resample-release (R3) sampling. In Andreas Krause, Emma Brunskill, Kyunghyun Cho, Barbara Engelhardt, Sivan Sabato, and Jonathan Scarlett (eds.), *Proceedings of the 40th International Conference on Machine Learning*, volume 202 of *Proceedings of Machine Learning Research*, pp. 7264–7302. PMLR, 23–29 Jul 2023. URL https://proceedings.mlr.press/v202/daw23a.html.

Tim De Ryck, Ameya D Jagtap, and Siddhartha Mishra. Error estimates for physics informed neural networks approximating the navier-stokes equations. *arXiv preprint arXiv:2203.09346*, 2022.

JW Dold. On asymptotic forms of reactive-diffusive runaway. *Proceedings of the Royal Society of London. Series A: Mathematical and Physical Sciences*, 433(1889):521–545, 1991.

Gintare Karolina Dziugaite and Daniel M Roy. Computing nonvacuous generalization bounds for deep (stochastic) neural networks with many more parameters than training data. *arXiv preprint arXiv:1703.11008*, 2017.

Weinan E, Jiequn Han, and Arnulf Jentzen. Algorithms for solving high dimensional PDEs: from nonlinear monte carlo to machine learning. *Nonlinearity*, 35(1):278–310, dec 2021. doi: 10.1088/1361-6544/ac337f. URL https://doi.org/10.1088%2F1361-6544%2Fac337f.

Hamidreza Eivazi, Mojtaba Tahani, Philipp Schlatter, and Ricardo Vinuesa. Physics-informed neural networks for solving reynolds-averaged navier–stokes equations. *Physics of Fluids*, 34(7): 075117, jul 2022. doi: 10.1063/5.0095270. URL https://doi.org/10.1063%2F5.0095270.

Tarek M. Elgindi. Finite-time singularity formation for $C^{1,\alpha}$ solutions to the incompressible Euler equations on $\mathbb{R}^3$. *Annals of Mathematics*, 194(3):647 – 727, 2021. doi: 10.4007/annals.2021.194.3.2. URL https://doi.org/10.4007/annals.2021.194.3.2.

N. Benjamin Erichson, Michael Muehlebach, and Michael W. Mahoney. Physics-informed autoencoders for lyapunov-stable fluid flow prediction, 2019.

Yuwei Fan, Cindy Orozco Bohorquez, and Lexing Ying. Bcr-net: A neural network based on the nonstandard wavelet form. *Journal of Computational Physics*, 384:1–15, 2019.

Hiroshi Fujita. On the blowing up of solutions of the cauchy problem for $u_1 + \delta u + u^{1+\alpha}$. 1966. URL https://api.semanticscholar.org/CorpusID:118871869.

Hiroshi Fujita. On the nonlinear equations $\Delta u + e^u = 0$ and $\partial v/\partial t = \Delta v + e^v$. *Bulletin of the American Mathematical Society*, 75(1):132 – 135, 1969.

Siming He and Eitan Tadmor. Suppressing chemotactic blow-up through a fast splitting scenario on the plane. *Archive for Rational Mechanics and Analysis*, 232:951–986, 2019.

Miguel A Herrero and JJL Velázquez. Plane structures in thermal runaway. *Israel Journal of Mathematics*, 81:321–341, 1993.

Miguel A. Herrero and Juan J. L. Velazquez. A blow-up mechanism for a chemotaxis model. *Annali della Scuola Normale Superiore di Pisa - Classe di Scienze*, Ser. 4, 24(4):633–683, 1997. URL http://www.numdam.org/item/ASNSP_1997_4_24_4_633_0/.

Zheyuan Hu, Ameya D. Jagtap, George Em Karniadakis, and Kenji Kawaguchi. When do extended physics-informed neural networks (XPINNs) improve generalization? *SIAM Journal on Scientific Computing*, 44(5):A3158–A3182, sep 2022a. doi: 10.1137/21m1447039. URL https://doi.org/10.1137%2F21m1447039.

Zheyuan Hu, Ameya D. Jagtap, George Em Karniadakis, and Kenji Kawaguchi. When do extended physics-informed neural networks (xpinns) improve generalization? *SIAM Journal on Scientific Computing*, 44(5):A3158–A3182, 2022b. doi: 10.1137/21M1447039. URL https://doi.org/10.1137/21M1447039.

Antony Jameson, Luigi Martinelli, and J Vassberg. Using computational fluid dynamics for aerodynamics–a critical assessment. In *Proceedings of ICAS*, pp. 2002–1, 2002.

Claes Johnson and Anders Szepessy. On the convergence of a finite element method for a nonlinear hyperbolic conservation law. *Mathematics of Computation - Math. Comput.*, 49:427–427, 10 1987. doi: 10.2307/2008320.

Eurika Kaiser, J. Nathan Kutz, and Steven L. Brunton. Data-driven discovery of koopman eigenfunctions for control, 2021.

Karniadakis, G.E., and Kevrekidis. Physics-informed machine learning, 2021.

Nikola Kovachki, Zongyi Li, Burigede Liu, Kamyar Azizzadenesheli, Kaushik Bhattacharya, Andrew Stuart, and Anima Anandkumar. Neural operator: Learning maps between function spaces with applications to pdes. *Journal of Machine Learning Research*, 24(89):1–97, 2023. URL http://jmlr.org/papers/v24/21-1524.html.

Aditi Krishnapriyan, Amir Gholami, Shandian Zhe, Robert Kirby, and Michael W Mahoney. Characterizing possible failure modes in physics-informed neural networks. *Advances in Neural Information Processing Systems*, 34:26548–26560, 2021.

A. A. Lacey. Thermal runaway in a non-local problem modelling ohmic heating. part ii: General proof of blow-up and asymptotics of runaway. *European Journal of Applied Mathematics*, 6(3): 201–224, 1995. doi: 10.1017/S0956792500001807.

AA Lacey. Mathematical analysis of thermal runaway for spatially inhomogeneous reactions. *SIAM Journal on Applied Mathematics*, 43(6):1350–1366, 1983.

I.E. Lagaris, A. Likas, and D.I. Fotiadis. Artificial neural networks for solving ordinary and partial differential equations. *IEEE Transactions on Neural Networks*, 9(5):987–1000, 1998. doi: 10.1109/72.712178. URL https://doi.org/10.1109%2F72.712178.

Zaharaddeen Lawal, Hayati Yassin, Daphne Teck Ching Lai, and Azam Idris. Physics-informed neural network (pinn) evolution and beyond: A systematic literature review and bibliometric analysis. *Big Data and Cognitive Computing*, 11 2022. doi: 10.3390/bdcc6040140.

Zongyi Li, Miguel Liu-Schiaffini, Nikola Kovachki, Burigede Liu, Kamyar Azizzadenesheli, Kaushik Bhattacharya, Andrew Stuart, and Anima Anandkumar. Learning dissipative dynamics in chaotic systems, 2022.

Yuandan Lin, Eduardo D. Sontag, and Yuan Wang. A smooth converse lyapunov theorem for robust stability. *SIAM Journal on Control and Optimization*, 34(1):124–160, 1996. doi: 10.1137/S0363012993259981. URL https://doi.org/10.1137/S0363012993259981.

Lu Lu, Pengzhan Jin, Guofei Pang, Zhongqiang Zhang, and George Em Karniadakis. Learning nonlinear operators via DeepONet based on the universal approximation theorem of operators. *Nature Machine Intelligence*, 3(3):218–229, mar 2021. doi: 10.1038/s42256-021-00302-5. URL https://doi.org/10.1038%2Fs42256-021-00302-5.

Lu Lu, Xuhui Meng, Shengze Cai, Zhiping Mao, Somdatta Goswami, Zhongqiang Zhang, and George Em Karniadakis. A comprehensive and fair comparison of two neural operators (with practical extensions) based on fair data. *Computer Methods in Applied Mechanics and Engineering*, 393:114778, 2022. ISSN 0045-7825. doi: https://doi.org/10.1016/j.cma.2022.114778. URL https://www.sciencedirect.com/science/article/pii/S0045782522001207.

Guo Luo and Thomas Y. Hou. Toward the finite-time blowup of the 3d axisymmetric euler equations: A numerical investigation. *Multiscale Modeling & Simulation*, 12(4):1722–1776, 2014a. doi: 10.1137/140966411. URL https://doi.org/10.1137/140966411.

Guo Luo and Thomas Y. Hou. Potentially singular solutions of the 3d axisymmetric euler equations. *Proceedings of the National Academy of Sciences*, 111(36):12968–12973, 2014b. doi: 10.1073/pnas.1405238111. URL https://www.pnas.org/doi/abs/10.1073/pnas.1405238111.

Siddhartha Mishra and Roberto Molinaro. Estimates on the generalization error of physics-informed neural networks for approximating PDEs. *IMA Journal of Numerical Analysis*, 43(1):1–43, 01 2022. ISSN 0272-4979. doi: 10.1093/imanum/drab093. URL https://doi.org/10.1093/imanum/drab093.

Anirbit Mukherjee. *A study of the mathematics of deep learning*. PhD thesis, The Johns Hopkins University, 2020.

Ramchandran Muthukumar and Jeremias Sulam. Sparsity-aware generalization theory for deep neural networks. In Gergely Neu and Lorenzo Rosasco (eds.), *Proceedings of Thirty Sixth Conference on Learning Theory*, volume 195 of *Proceedings of Machine Learning Research*, pp. 5311–5342. PMLR, 12–15 Jul 2023. URL https://proceedings.mlr.press/v195/muthukumar23a.html.

Haim Nessyahu and Eitan Tadmor. The convergence rate of approximate solutions for nonlinear scalar conservation laws. *SIAM Journal on Numerical Analysis*, 29(6):1505–1519, 1992. doi: 10.1137/0729087. URL https://doi.org/10.1137/0729087.

Behnam Neyshabur, Srinadh Bhojanapalli, and Nathan Srebro. A pac-bayesian approach to spectrally-normalized margin bounds for neural networks. *arXiv preprint arXiv:1707.09564*, 2017.

Behnam Neyshabur, Zhiyuan Li, Srinadh Bhojanapalli, Yann LeCun, and Nathan Srebro. Towards understanding the role of over-parametrization in generalization of neural networks. *arXiv preprint arXiv:1805.12076*, 2018.

A. Pazy. *Some Nonlinear Evolution Equations*, pp. 183–205. Springer New York, New York, NY, 1983. ISBN 978-1-4612-5561-1. doi: 10.1007/978-1-4612-5561-1_6. URL https://doi.org/10.1007/978-1-4612-5561-1_6.

Nasim Rahaman, Aristide Baratin, Devansh Arpit, Felix Draxler, Min Lin, Fred Hamprecht, Yoshua Bengio, and Aaron Courville. On the spectral bias of neural networks. In *International Conference on Machine Learning*, pp. 5301–5310. PMLR, 2019.

Maziar Raissi, Paris Perdikaris, and George E Karniadakis. Physics-informed neural networks: A deep learning framework for solving forward and inverse problems involving nonlinear partial differential equations. *Journal of Computational physics*, 378:686–707, 2019.

Bogdan Raonić, Roberto Molinaro, Tobias Rohner, Siddhartha Mishra, and Emmanuel de Bezenac. Convolutional neural operators. *arXiv preprint arXiv:2302.01178*, 2023.

Franz M Rohrhofer, Stefan Posch, Clemens Gößnitzer, and Bernhard C Geiger. On the role of fixed points of dynamical systems in training physics-informed neural networks. *arXiv preprint arXiv:2203.13648*, 2022.

Cristopher Salvi, Maud Lemercier, and Andris Gerasimovics. Neural stochastic pdes: Resolution-invariant learning of continuous spatiotemporal dynamics, 2022.

Justin Sirignano and Konstantinos Spiliopoulos. Dgm: A deep learning algorithm for solving partial differential equations. *Journal of computational physics*, 375:1339–1364, 2018.

A. M. Stuart and M. S. Floater. On the computation of blow-up. *European Journal of Applied Mathematics*, 1(1):47–71, 1990. doi: 10.1017/S095679250000005X.

Eitan Tadmor. Local error estimates for discontinuous solutions of nonlinear hyperbolic equations. *SIAM Journal on Numerical Analysis*, 28(4):891–906, 1991. doi: 10.1137/0728048. URL https://doi.org/10.1137/0728048.

Yuya Tanaka. Finite-time blow-up in a two species chemotaxis-competition model with degenerate diffusion. *arXiv preprint arXiv:2304.13421*, 2023.

Terence Tao. Finite time blowup for lagrangian modifications of the three-dimensional euler equation. *Annals of PDE*, 2:1–79, 2016a.

Terence Tao. Finite time blowup for an averaged three-dimensional navier-stokes equation. *Journal of the American Mathematical Society*, 29(3):601–674, 2016b.

Nils Wandel, Michael Weinmann, and Reinhard Klein. Teaching the incompressible navier–stokes equations to fast neural surrogate models in three dimensions. *Physics of Fluids*, 33(4):047117, apr 2021. doi: 10.1063/5.0047428. URL https://doi.org/10.1063%2F5.0047428.

Chuwei Wang, Shanda Li, Di He, and Liwei Wang. Is l^2 physics informed loss always suitable for training physics informed neural network? *Advances in Neural Information Processing Systems*, 35:8278–8290, 2022a.

Rui Wang, Karthik Kashinath, Mustafa Mustafa, Adrian Albert, and Rose Yu. Towards physics-informed deep learning for turbulent flow prediction, 2020.

Sifan Wang, Yujun Teng, and Paris Perdikaris. Understanding and mitigating gradient flow pathologies in physics-informed neural networks. *SIAM Journal on Scientific Computing*, 43(5): A3055–A3081, 2021a. doi: 10.1137/20M1318043. URL https://doi.org/10.1137/20M1318043.

Sifan Wang, Hanwen Wang, and Paris Perdikaris. Learning the solution operator of parametric partial differential equations with physics-informed deeponets. *Science Advances*, 7(40):eabi8605, 2021b. doi: 10.1126/sciadv.abi8605. URL https://www.science.org/doi/abs/10.1126/sciadv.abi8605.

Sifan Wang, Shyam Sankaran, and Paris Perdikaris. Respecting causality is all you need for training physics-informed neural networks. *arXiv preprint arXiv:2203.07404*, 2022b.

Sifan Wang, Xinling Yu, and Paris Perdikaris. When and why pinns fail to train: A neural tangent kernel perspective. *Journal of Computational Physics*, 449:110768, 2022c. ISSN 0021-9991. doi: https://doi.org/10.1016/j.jcp.2021.110768. URL https://www.sciencedirect.com/science/article/pii/S002199912100663X.

Yongji Wang, Ching-Yao Lai, Javier Gómez-Serrano, and Tristan Buckmaster. Asymptotic self-similar blow up profile for 3-d euler via physics-informed neural networks, 2022d.

Aurel Wintner. The non-local existence problem of ordinary differential equations. *American Journal of Mathematics*, 67(2):277–284, 1945. ISSN 00029327, 10806377. URL http://www.jstor.org/stable/2371729.

Bing Yu et al. The deep ritz method: a deep learning-based numerical algorithm for solving variational problems. *Communications in Mathematics and Statistics*, 6(1):1–12, 2018.

A Proofs for the Main Theorems

A.1 Proof of Theorem 3.1

Let $\boldsymbol{u}$ be the actual solution of the (d+1)-dimensional Burgers' PDE and $\boldsymbol{u}_\theta$ the predicted solution by the PINN with parameters θ. Let's define

$$f(\boldsymbol{u}) \coloneqq \frac{\|\boldsymbol{u}\|_2^2}{2}$$
$$\hat{\boldsymbol{u}} \coloneqq \boldsymbol{u}_\theta - \boldsymbol{u}$$

Then we can write the (d+1)-dimenional Burgers' and it's residual as

$$\partial_t \boldsymbol{u} + (\boldsymbol{u} \cdot \nabla)\boldsymbol{u} = 0 \tag{17}$$
$$\mathcal{R}_{\text{pde}} \coloneqq \partial_t \boldsymbol{u}_\theta + (\boldsymbol{u}_\theta \cdot \nabla)\boldsymbol{u}_\theta \tag{18}$$

Now multiplying (18) with $\boldsymbol{u}_\theta$ on both sides we get

$$\boldsymbol{u}_\theta \cdot \mathcal{R}_{\text{pde}} = \partial_t f(\boldsymbol{u}_\theta) + \boldsymbol{u}_\theta \cdot \nabla f(\boldsymbol{u}_\theta) \tag{19}$$

Similarly, multiplying both sides of (17) with $\boldsymbol{u}$ we get

$$\partial_t f(\boldsymbol{u}) + \boldsymbol{u} \cdot \nabla f(\boldsymbol{u}) = 0 \tag{20}$$

Some calculation on (17) and (18) yields

$$\begin{aligned}
&\boldsymbol{u} \cdot [(\partial_t \boldsymbol{u}_\theta + (\boldsymbol{u}_\theta \cdot \nabla)\boldsymbol{u}_\theta - \mathcal{R}_{\text{pde}}) - (\partial_t \boldsymbol{u} + (\boldsymbol{u} \cdot \nabla)\boldsymbol{u})] = -\hat{\boldsymbol{u}} \cdot [\partial_t \boldsymbol{u} + (\boldsymbol{u} \cdot \nabla)\boldsymbol{u}] \\
\implies &\partial_t(\boldsymbol{u} \cdot \hat{\boldsymbol{u}}) + \boldsymbol{u} \cdot ((\boldsymbol{u}_\theta \cdot \nabla)\boldsymbol{u}_\theta) - \boldsymbol{u} \cdot ((\boldsymbol{u} \cdot \nabla)\boldsymbol{u}) - \boldsymbol{u} \cdot \mathcal{R}_{\text{pde}} = -\hat{\boldsymbol{u}} \cdot ((\boldsymbol{u} \cdot \nabla)\boldsymbol{u}) \\
\implies &\partial_t(\boldsymbol{u} \cdot \hat{\boldsymbol{u}}) + \boldsymbol{u} \cdot ((\boldsymbol{u}_\theta \cdot \nabla)\boldsymbol{u}_\theta) - \boldsymbol{u} \cdot \nabla f(\boldsymbol{u}) - \boldsymbol{u} \cdot \mathcal{R}_{\text{pde}} = -\hat{\boldsymbol{u}} \cdot ((\boldsymbol{u} \cdot \nabla)\boldsymbol{u})
\end{aligned} \tag{21}$$

Let

$$S \coloneqq \frac{1}{2}\hat{\boldsymbol{u}} \cdot \hat{\boldsymbol{u}} \tag{22}$$

$$\begin{aligned}
\implies \partial_t S &= \partial_t f(\boldsymbol{u}_\theta) - \partial_t f(\boldsymbol{u}) - \partial_t(\boldsymbol{u} \cdot \hat{\boldsymbol{u}}) \\
&= [\boldsymbol{u}_\theta \cdot \mathcal{R}_{\text{pde}} - \boldsymbol{u}_\theta \cdot \nabla f(\boldsymbol{u}_\theta)] + [\boldsymbol{u} \cdot \nabla f(\boldsymbol{u})] \\
&\quad - [-\boldsymbol{u} \cdot ((\boldsymbol{u}_\theta \cdot \nabla)\boldsymbol{u}_\theta) + \boldsymbol{u} \cdot \nabla f(\boldsymbol{u}) + \boldsymbol{u} \cdot \mathcal{R}_{\text{pde}} - \hat{\boldsymbol{u}} \cdot ((\boldsymbol{u} \cdot \nabla)\boldsymbol{u})] \\
&= \hat{\boldsymbol{u}} \cdot \mathcal{R}_{\text{pde}} - \boldsymbol{u}_\theta \cdot \nabla f(\boldsymbol{u}_\theta) + \boldsymbol{u} \cdot ((\boldsymbol{u}_\theta \cdot \nabla)\boldsymbol{u}_\theta) + \hat{\boldsymbol{u}} \cdot ((\boldsymbol{u} \cdot \nabla)\boldsymbol{u}) \\
&= \hat{\boldsymbol{u}} \cdot \mathcal{R}_{\text{pde}} + \hat{\boldsymbol{u}} \cdot ((\boldsymbol{u} \cdot \nabla)\boldsymbol{u} - (\boldsymbol{u}_\theta \cdot \nabla)\boldsymbol{u}_\theta)
\end{aligned}$$

here we represent the spatial domain $[0,1] \times [0,1]$ by D and use Ω to represent the $D \times [-\frac{1}{\sqrt{2}} + \delta, \delta]$. We then define

$$\mathcal{T} \coloneqq \hat{\boldsymbol{u}} \cdot ((\boldsymbol{u} \cdot \nabla)\boldsymbol{u}) \tag{23}$$
$$\tilde{H} \coloneqq \hat{\boldsymbol{u}} \cdot ((\boldsymbol{u}_\theta \cdot \nabla)\boldsymbol{u}_\theta) \tag{24}$$

And this leads to,

$$\partial_t S + \tilde{H} = \hat{\boldsymbol{u}} \cdot \mathcal{R}_{\text{pde}} + \mathcal{T} \tag{25}$$

Thus we have the inequalities,

$$\begin{aligned}
\int_D \partial_t \|\hat{\boldsymbol{u}}\|_2^2 \,\mathrm{d}\boldsymbol{x} \le &\int_D \|\hat{\boldsymbol{u}}\|_2^2 \,\mathrm{d}\boldsymbol{x} + \int_D \|\mathcal{R}_{pde}\|_2^2 \,\mathrm{d}\boldsymbol{x} \\
&+ 2\int_D \hat{\boldsymbol{u}} \cdot ((\boldsymbol{u} \cdot \nabla)\boldsymbol{u}) \,\mathrm{d}\boldsymbol{x} - 2\int_D \hat{\boldsymbol{u}} \cdot ((\boldsymbol{u}_\theta \cdot \nabla)\boldsymbol{u}_\theta) \,\mathrm{d}\boldsymbol{x} \\
&\le \int_D \|\hat{\boldsymbol{u}}\|_2^2 \,\mathrm{d}\boldsymbol{x} + \int_D \|\mathcal{R}_{pde}\|_2^2 \,\mathrm{d}\boldsymbol{x} \\
&+ 2d^2 \|\nabla \boldsymbol{u}\|_{L^\infty(\Omega)} \int_D \|\boldsymbol{u}\|_2 \|\hat{\boldsymbol{u}}\|_2 \,\mathrm{d}\boldsymbol{x} + 2d^2 \|\nabla \boldsymbol{u}_\theta\|_{L^\infty(\Omega)} \int_D \|\boldsymbol{u}_\theta\|_2 \|\hat{\boldsymbol{u}}\|_2 \,\mathrm{d}\boldsymbol{x} \\
&\le \int_D \|\hat{\boldsymbol{u}}\|_2^2 \,\mathrm{d}\boldsymbol{x} + \int_D \|\mathcal{R}_{pde}\|_2^2 \,\mathrm{d}\boldsymbol{x} \\
&+ d^2 \|\nabla \boldsymbol{u}\|_{L^\infty(\Omega)} \int_D \left[\|\boldsymbol{u}\|_2^2 + \|\hat{\boldsymbol{u}}\|_2^2\right] \mathrm{d}\boldsymbol{x} + d^2 \|\nabla \boldsymbol{u}_\theta\|_{L^\infty(\Omega)} \int_D \left[\|\boldsymbol{u}_\theta\|_2^2 + \|\hat{\boldsymbol{u}}\|_2^2\right] \mathrm{d}\boldsymbol{x}
\end{aligned}$$

$$
\begin{aligned}
&\leq \Big[1 + d^2 \|\nabla \boldsymbol{u}\|_{L^\infty(\Omega)} + d^2 \|\nabla \boldsymbol{u}_\theta\|_{L^\infty(\Omega)}\Big] \int_D \|\hat{\boldsymbol{u}}\|_2^2 \,\mathrm{d}\boldsymbol{x} \\
&+ \int_D \|\mathcal{R}_{pde}\|_2^2 \,\mathrm{d}\boldsymbol{x} + d^2 \|\nabla \boldsymbol{u}\|_{L^\infty(\Omega)} \int_D \|\boldsymbol{u}\|_2^2 \,\mathrm{d}\boldsymbol{x} + d^2 \|\nabla \boldsymbol{u}_\theta\|_{L^\infty(\Omega)} \int_D \|\boldsymbol{u}_\theta\|_2^2 \,\mathrm{d}\boldsymbol{x} \\
&\leq C_1 \int_D \|\hat{\boldsymbol{u}}\|_2^2 \,\mathrm{d}\boldsymbol{x} + \int_D \|\mathcal{R}_{pde}\|_2^2 \,\mathrm{d}\boldsymbol{x} \\
&+ d^2 \|\nabla \boldsymbol{u}\|_{L^\infty(\Omega)} \int_D \|\boldsymbol{u}\|_2^2 \,\mathrm{d}\boldsymbol{x} + d^2 \|\nabla \boldsymbol{u}_\theta\|_{L^\infty(\Omega)} \int_D \|\boldsymbol{u}_\theta\|_2^2 \,\mathrm{d}\boldsymbol{x} \qquad (26)
\end{aligned}
$$

where

$$
\begin{aligned}
C_1 &= d^2 \|\nabla \boldsymbol{u}_\theta\|_{L^\infty(\Omega)} \\
&\quad + 1 + d^2 \|\nabla \boldsymbol{u}\|_{L^\infty(\Omega)}
\end{aligned}
$$

Lets define the domain $D \times [-\frac{1}{\sqrt{2}} + \delta, \tilde{\delta}]$ by $\tilde{\Omega}$ where $\tilde{\delta} \in [-\frac{1}{\sqrt{2}} + \delta, \delta)$.

Integrating over $\tilde{\Omega}$ we get

$$
\begin{aligned}
\int_{\tilde{\Omega}} \partial_t \|\hat{\boldsymbol{u}}\|_2^2 \,\mathrm{d}\boldsymbol{x}\,\mathrm{d}t &\leq C_1 \int_{\tilde{\Omega}} \|\hat{\boldsymbol{u}}\|_2^2 \,\mathrm{d}\boldsymbol{x}\,\mathrm{d}t + \int_{\tilde{\Omega}} \|\mathcal{R}_{pde}\|_2^2 \,\mathrm{d}\boldsymbol{x}\,\mathrm{d}t \\
&+ d^2 \|\nabla \boldsymbol{u}\|_{L^\infty(\Omega)} \int_{\tilde{\Omega}} \|\boldsymbol{u}\|_2^2 \,\mathrm{d}\boldsymbol{x}\,\mathrm{d}t + d^2 \|\nabla \boldsymbol{u}_\theta\|_{L^\infty(\Omega)} \int_{\tilde{\Omega}} \|\boldsymbol{u}_\theta\|_2^2 \,\mathrm{d}\boldsymbol{x}\,\mathrm{d}t \\
&\leq \int_D \|\mathcal{R}_t\|_2^2 \,\mathrm{d}\boldsymbol{x} + C_1 \int_{\tilde{\Omega}} \|\hat{\boldsymbol{u}}\|_2^2 \,\mathrm{d}\boldsymbol{x}\,\mathrm{d}t + \int_{\tilde{\Omega}} \|\mathcal{R}_{pde}\|_2^2 \,\mathrm{d}\boldsymbol{x}\,\mathrm{d}t \\
&+ d^2 \|\nabla \boldsymbol{u}\|_{L^\infty(\Omega)} \int_{\tilde{\Omega}} \|\boldsymbol{u}\|_2^2 \,\mathrm{d}\boldsymbol{x}\,\mathrm{d}t + d^2 \|\nabla \boldsymbol{u}_\theta\|_{L^\infty(\Omega)} \int_{\tilde{\Omega}} \|\boldsymbol{u}_\theta\|_2^2 \,\mathrm{d}\boldsymbol{x}\,\mathrm{d}t \\
&\leq \int_D \|\mathcal{R}_t\|_2^2 \,\mathrm{d}\boldsymbol{x} + C_1 \int_{\Omega} \|\hat{\boldsymbol{u}}\|_2^2 \,\mathrm{d}\boldsymbol{x}\,\mathrm{d}t + \int_{\Omega} \|\mathcal{R}_{pde}\|_2^2 \,\mathrm{d}\boldsymbol{x}\,\mathrm{d}t \\
&+ d^2 \|\nabla \boldsymbol{u}\|_{L^\infty(\Omega)} \int_{\Omega} \|\boldsymbol{u}\|_2^2 \,\mathrm{d}\boldsymbol{x}\,\mathrm{d}t + d^2 \|\nabla \boldsymbol{u}_\theta\|_{L^\infty(\Omega)} \int_{\Omega} \|\boldsymbol{u}_\theta\|_2^2 \,\mathrm{d}\boldsymbol{x}\,\mathrm{d}t \\
&\leq C_1 \int_{\tilde{\Omega}} \|\hat{\boldsymbol{u}}\|_2^2 \,\mathrm{d}\boldsymbol{x}\,\mathrm{d}t + C_2 \qquad (27)
\end{aligned}
$$

where,

$$
\begin{aligned}
C_2 = &\int_D \|\mathcal{R}_t\|_2^2 \,\mathrm{d}\boldsymbol{x} + \int_{\tilde{\Omega}} \|\mathcal{R}_{pde}\|_2^2 \,\mathrm{d}\boldsymbol{x}\,\mathrm{d}t + d^2 \|\nabla \boldsymbol{u}_\theta\|_{L^\infty(\Omega)} \int_{\tilde{\Omega}} \|\boldsymbol{u}_\theta\|_2^2 \,\mathrm{d}\boldsymbol{x}\,\mathrm{d}t \\
&+ d^2 \|\nabla \boldsymbol{u}\|_{L^\infty(\Omega)} \int_{\tilde{\Omega}} \|\boldsymbol{u}\|_2^2 \,\mathrm{d}\boldsymbol{x}\,\mathrm{d}t
\end{aligned}
$$

Applying Gronwall's inequality on (27) we get

$$
\int_D \left\|\hat{\boldsymbol{u}}(\boldsymbol{x}, \tilde{\delta})\right\|_2^2 \mathrm{d}\boldsymbol{x} \leq C_2 + \int_{-\frac{1}{\sqrt{2}}+\delta}^{\tilde{\delta}} C_2 C_1 e^{\int_t^\delta C_1 \,\mathrm{d}s} \,\mathrm{d}t \leq C_2 \left[1 + \int_{-\frac{1}{\sqrt{2}}+\delta}^{\tilde{\delta}} C_1 e^{\frac{C_1}{\sqrt{2}}} \,\mathrm{d}t\right] \qquad (28)
$$

Integrating (28) over $\mathrm{d}\tilde{\delta}$ we get

$$
\begin{aligned}
\int_\Omega \left\|\hat{\boldsymbol{u}}(\boldsymbol{x}, \tilde{\delta})\right\|_2^2 \mathrm{d}\boldsymbol{x}\,\mathrm{d}\tilde{\delta} &\leq C_2 \int_{\frac{-1}{\sqrt{2}}+\delta}^{\delta} \left[1 + \int_{-\frac{1}{\sqrt{2}}+\delta}^{\tilde{\delta}} C_1 e^{\frac{C_1}{\sqrt{2}}} \,\mathrm{d}t\right] \mathrm{d}\tilde{\delta} \\
&\leq C_2 \left[\frac{-1}{\sqrt{2}} + \int_{\frac{-1}{\sqrt{2}}+\delta}^{\delta} \int_{-\frac{1}{\sqrt{2}}+\delta}^{\tilde{\delta}} C_1 e^{\frac{C_1}{\sqrt{2}}} \,\mathrm{d}t\,\mathrm{d}\tilde{\delta}\right] \\
&\leq C_2 \left[\frac{-1}{\sqrt{2}} + \frac{C_1}{4} e^{\frac{C_1}{\sqrt{2}}}\right] \\
\implies \log\left(\int_\Omega \left\|\hat{\boldsymbol{u}}(\boldsymbol{x}, \tilde{\delta})\right\|_2^2 \mathrm{d}\boldsymbol{x}\,\mathrm{d}\tilde{\delta}\right) &\leq \log\left(\frac{C_1 C_2}{4}\right) + \frac{C_1}{\sqrt{2}} \qquad (29)
\end{aligned}
$$

A.2 USEFUL LEMMAS

Lemma A.1.

$$
\begin{aligned}
\int_D p \cdot ((q \cdot \nabla) r) dx &= \int_D \left[\sum_{i=1}^{d} p_i \left(q \cdot \nabla r_i \right) \right] dx \\
&\leq \int_D \left[\sum_{i=1}^{d} \|p\|_2 \left(\|q\|_2 \|\nabla r_i\|_2 \right) \right] dx \\
&\leq \int_D \|p\|_2 \|q\|_2 \left[\sum_{i=1}^{d} \|\nabla r_i\|_2 \right] dx \\
&\leq \int_D \|p\|_2 \|q\|_2 \left[\sum_{i=1}^{d} d \|\nabla r\|_{L^\infty(\Omega)} \right] dx \\
&\leq d^2 \|\nabla r\|_{L^\infty(\Omega)} \int_D \|p\|_2 \|q\|_2 dx
\end{aligned} \tag{30}
$$

A.3 Proof of Theorem 3.2

Proof. We define

$$f(u) = \frac{u^2}{2}$$

which means the first equation in (6) can be written as

$$u_t + f(u)_x = 0 \tag{31}$$

Then we define the entropy flux function as

$$\mathcal{Q}(u) = \int_a^u s f'(s) ds \quad \text{for any } a \in \mathbb{R}$$

Let $\hat{u} = u^* - u$. From (7) we get

$$\partial_t \left(\frac{(u^*)^2}{2} \right) + \partial_x \mathcal{Q}(u^*) = u^* \mathcal{R}_{int,\theta*} \tag{32}$$

and from (31) we obtain

$$\partial_t \left(\frac{u^2}{2} \right) + \partial_x \mathcal{Q}(u) = 0 \tag{33}$$

Some calculation on (31) and (7) yields

$$\partial_t(u\hat{u}) + \partial_x(u(f(u^*) - f(u))) = [f(u^*) - f(u) - \hat{u}f'(u)]u_x + u\mathcal{R}_{int,\theta^*} \tag{34}$$

Subtracting (34) and (33) from (32) we get

$$\partial_t S(u, u^*) + \partial_x H(u, u^*) = \hat{u}\mathcal{R}_{int,\theta^*} + T_1 \tag{35}$$

with,

$$\begin{aligned} S(u,u^*) &:= \frac{(u^*)^2}{2} - \frac{u^2}{2} - \hat{u}u = \frac{1}{2}\hat{u}^2, \\ H(u,u^*) &:= \mathcal{Q}(u^*) - \mathcal{Q}(u) - u(f(u^*) - f(u)), \\ T_1 &= -\left[f(u^*) - f(u) - f'(u)\hat{u}\right] u_x \end{aligned}$$

As flux f is smooth, we can apply Taylor expansion[5] on T_1 and expand $f(u^*)$ at u,

$$\begin{aligned} T_1 &= -\left[\cancel{f(u)} + \cancel{f'(u)\hat{u}} + \frac{f''(u+\gamma(u^*-u))}{2}(u^*-u)^2 - \cancel{f(u)} - \cancel{f'(u)\hat{u}}\right] u_x \\ &\quad [\text{ where } \gamma \in (0,1)] \\ &= -\frac{1}{2}\, \cancelto{1}{f''(u+\gamma(u^*-u))}\, \hat{u}^2 u_x \\ &= -\frac{1}{2}\hat{u}^2 u_x \end{aligned}$$

Hence it can be reasonably bounded by

$$|T_1| \le \|u_x\|_{L^\infty} \hat{u}^2 \tag{36}$$

[5] with the Lagrange form of the remainder

where C_{u_x} is given by $C_{u_x} = \|u_x\|_{L^\infty}$. Next, we integrate (35) over the domain (-1,1)

$$\begin{aligned}
\int_{-1}^{1} \partial_t S(u,u^*)dx &= -\int_{-1}^{1} \partial_x H(u,u^*)dx + \int_{-1}^{1} \hat{u}\mathcal{R}_{int,\theta^*}dx + \int_{-1}^{1} T_1 dx \\
\Rightarrow \frac{\mathrm{d}}{\mathrm{d}t}\int_{-1}^{1} \frac{\hat{u}^2(x,t)}{2}dx &\le H(u(-1,t),u^*(-1,t)) - H(u(1,t),u^*(1,t)) \\
&\quad + C_{u_x}\int_{-1}^{1} \hat{u}^2(x,t)dx + \int_{-1}^{1} \hat{u}(x,t)\mathcal{R}_{int,\theta^*}(x,t)dx \\
\Rightarrow \frac{\mathrm{d}}{\mathrm{d}t}\int_{-1}^{1} \hat{u}^2(x,t)dx &\le 2H(u(-1,t),u^*(-1,t)) - 2H(u(1,t),u^*(1,t)) \\
&\quad + 2C_{u_x}\int_{-1}^{1} \hat{u}^2(x,t)dx + \int_{-1}^{1} (\mathcal{R}^2_{int,\theta^*}(x,t) + \hat{u}^2(x,t))dx \\
\Rightarrow \frac{\mathrm{d}}{\mathrm{d}t}\int_{-1}^{1} \hat{u}^2(x,t)dx &\le 2H(u(-1,t),u^*(-1,t)) - 2H(u(1,t),u^*(1,t)) \\
&\quad + C\int_{-1}^{1} \hat{u}^2(x,t)dx + \int_{-1}^{1} \mathcal{R}^2_{int,\theta^*}(x,t)dx
\end{aligned} \tag{37}$$

where $C = 1 + 2C_{u_x}$. We can estimate $H(u(1,t),u^*(1,t))$ using (6)

$$\begin{aligned}
H(u(1,t),u^*(1,t)) &= \mathcal{Q}(u^*(1,t)) - \mathcal{Q}(u(1,t)) - u(1,t)(f(u^*(1,t)) - f(u(1,t))) \\
&= \mathcal{Q}'(\gamma_1\mathcal{R}_{sb,1,\theta^*}(t))\mathcal{R}_{sb,1,\theta^*}(t) - \frac{u(1,t)}{2}\left[\hat{u}(1,t)\left[u^*(1,t)+u(1,t)\right]\right] \\
&\quad [\text{ for some } \gamma_1 \in (0,1) \text{ by the mean-value theorem}] \\
&= \gamma_1 f'(\gamma_1\mathcal{R}_{sb,1,\theta^*})\mathcal{R}^2_{sb,1,\theta^*}(t) - \frac{u(1,t)}{2}\left[\mathcal{R}_{sb,1,\theta^*} + 2u(1,t)\right]\mathcal{R}_{sb,1,\theta^*} \\
&= \gamma_1\left[f'(\gamma_1\mathcal{R}_{sb,1,\theta^*}) - \frac{u(1,t)}{2}\right]\mathcal{R}^2_{sb,1,\theta^*}(t) - u^2(1,t)\mathcal{R}_{sb,1,\theta^*} \\
&\le C_{2b}\mathcal{R}^2_{sb,1,\theta^*}(t) + u^2(1,t)|\mathcal{R}_{sb,1,\theta^*}| \\
&\quad \text{with } C_{2b} = C_{2b}(\|f'\|_\infty, \|u\|_{C^1([-1,1]\times[-1+\delta,\delta])})
\end{aligned}$$

Similarly we can estimate

$$H(u(-1,t),u^*(-1,t)) \le C_{2b}\mathcal{R}^2_{sb,-1,\theta^*}(t) + u^2(-1,t)|\mathcal{R}_{sb,-1,\theta^*}|$$

Now, we can integrate (37) over the time interval $[-1+\delta,\bar{\delta}]$ for any $\bar{\delta} \in [-1+\delta,\delta]$ and use the above inequalities along with (8)

$$\begin{aligned}
\int_{-1+\delta}^{\bar{\delta}} \frac{\mathrm{d}}{\mathrm{d}t}\int_{-1}^{1} \hat{u}^2(x,t)dxdt &\le \int_{-1+\delta}^{\bar{\delta}} (2H(u(-1,t),u^*(-1,t)) - 2H(u(1,t),u^*(1,t)))dt \\
&\quad + \int_{-1+\delta}^{\bar{\delta}} C\int_{-1}^{1} \hat{u}^2(x,t)dxdt + \int_{-1+\delta}^{\bar{\delta}}\int_{-1}^{1} \mathcal{R}^2_{int,\theta^*}(x,t)dxdt
\end{aligned}$$

$$\begin{aligned}
\Rightarrow \int_{-1}^{1} \hat{u}^2(x,\bar{\delta})dx &\le \int_{-1}^{1} \hat{u}^2(x,-1+\delta)dx + 2C_{2b}\left[\int_{-1+\delta}^{\delta} \mathcal{R}^2_{sb,-1,\theta^*}(t)dt + \int_{-1+\delta}^{\delta} \mathcal{R}^2_{sb,1,\theta^*}(t)dt\right] \\
&\quad + 2\left[\int_{-1+\delta}^{\delta} u^2(-1,t)|\mathcal{R}_{sb,-1,\theta^*}|dt + \int_{-1+\delta}^{\delta} u^2(1,t)|\mathcal{R}_{sb,1,\theta^*}|dt\right] \\
&\quad + C\int_{-1+\delta}^{\bar{\delta}}\int_{-1}^{1} \hat{u}^2(x,t)dxdt + \int_{-1+\delta}^{\delta}\int_{-1}^{1} \mathcal{R}^2_{int,\theta^*}(x,t)dxdt
\end{aligned}$$

$$\begin{aligned}
\Rightarrow \int_{-1}^{1} \hat{u}^2(x,\bar{\delta})dx \le & \int_{-1}^{1} \mathcal{R}_{tb,\theta^*}(x)dx + 2C_{2b}\left[\int_{-1+\delta}^{\delta} \mathcal{R}^2_{sb,-1,\theta^*}(t)dt + \int_{-1+\delta}^{\delta} \mathcal{R}^2_{sb,1,\theta^*}(t)dt\right] \\
& + 2C_{1b}\left[\int_{-1+\delta}^{\delta} |\mathcal{R}_{sb,-1,\theta^*}|dt + \int_{-1+\delta}^{\delta} |\mathcal{R}_{sb,1,\theta^*}|dt\right] \\
& + C\int_{-1+\delta}^{\bar{\delta}}\int_{-1}^{1} \hat{u}^2(x,t)dxdt + \int_{-1+\delta}^{\delta}\int_{-1}^{1} \mathcal{R}^2_{int,\theta^*}(x,t)dxdt \\
& \text{where } C_{1b} = C_{1b}(\|u(1,t)\|_{L^\infty}) \\
& \le \int_{-1}^{1} \mathcal{R}_{tb,\theta^*}(x)dx + 2\bar{C}_{2b}\left[\int_{-1+\delta}^{\delta} \mathcal{R}^2_{sb,-1,\theta^*}(t)dt + \int_{-1+\delta}^{\delta} \mathcal{R}^2_{sb,1,\theta^*}(t)dt\right] \\
& + 2C_{1b}(\delta-(\delta-1))^{\frac{1}{2}}\left[\left(\int_{-1+\delta}^{\delta} \mathcal{R}^2_{sb,-1,\theta^*}dt\right)^{\frac{1}{2}} + \left(\int_{-1+\delta}^{\delta} \mathcal{R}^2_{sb,1,\theta^*}dt\right)^{\frac{1}{2}}\right] \\
& + C\int_{-1+\delta}^{\bar{\delta}}\int_{-1}^{1} \hat{u}^2(x,t)dxdt + \int_{-1+\delta}^{\delta}\int_{-1}^{1} \mathcal{R}^2_{int,\theta^*}(x,t)dxdt \\
& \text{by using Holder's inequality} \\
& \le C_T + C\int_{-1+\delta}^{\bar{\delta}}\int_{-1}^{1} \hat{u}^2(x,t)dxdt
\end{aligned}$$

$$\begin{aligned}
\text{where } C_T = & \int_{-1}^{1} \mathcal{R}_{tb,\theta^*}(x)\,\mathrm{d}x + 2C_{2b}\left[\int_{-1+\delta}^{\delta} \mathcal{R}^2_{sb,-1,\theta^*}(t)\,\mathrm{d}t + \int_{-1+\delta}^{\delta} \mathcal{R}^2_{sb,1,\theta^*}(t)\,\mathrm{d}t\right] \\
+ & \int_{-1+\delta}^{\delta}\int_{-1}^{1} \mathcal{R}^2_{int,\theta^*}(x,t)\,\mathrm{d}x\,\mathrm{d}t + 2C_{1b}\left[\left(\int_{-1+\delta}^{\delta} \mathcal{R}^2_{sb,-1,\theta^*}\,\mathrm{d}t\right)^{\frac{1}{2}} + \left(\int_{-1+\delta}^{\delta} \mathcal{R}^2_{sb,1,\theta^*}\,\mathrm{d}t\right)^{\frac{1}{2}}\right] \qquad (38)
\end{aligned}$$

Using integral form of Grönwall's inequality on (38)

$$\int_{-1}^{1} \hat{u}^2(x,\bar{\delta})dx \le C_T + \int_{-1+\delta}^{\bar{\delta}} C_T C e^{\int_t^{\delta} C ds} dt \le \left[1 + \int_{-1+\delta}^{\bar{\delta}} Ce^C dt\right] C_T \qquad (39)$$

Integrating (39) over $\bar{\delta}$ together with the definition of generalization error (10) we get

$$\begin{aligned}
\int_{-1+\delta}^{\delta}\int_{-1}^{1} \hat{u}^2(x,\bar{\delta})dxd\bar{\delta} &\le C_T\int_{-1+\delta}^{\delta}\left[1 + \int_{-1+\delta}^{\bar{\delta}} Ce^C dt\right]d\bar{\delta} \\
\mathcal{E}_G^2 &\le \left[1 + Ce^C\right]C_T \qquad (40)
\end{aligned}$$

□

A.4 Making The Data Dependence Explicit in the bounds for $1+1$ Burgers' PDE

A.4.1 Quadrature Rule

Let' say we have a mapping $g : \mathbb{D} \to \mathbb{R}^m$ such that $g \in Z^* \subset L^p(\mathbb{D}, \mathbb{R}^m)$ and $\mathbb{D} \subset \mathbb{R}^{\bar{d}}$. Let's say we have an integral that we want to approximate

$$\bar{g} \coloneqq \int_{\mathbb{D}} g(y)\, dy \qquad (41)$$

where dy denotes the $\bar{d}$-dimensional Lebesgue measure. To approximate this integral by the quadrature rule we need (i) the quadrature points $y_i \in \mathbb{D}$ for $1 \le i \le N$ for some $N \in \mathbb{N}$ and (ii) weights w_i with $w_i \in \mathbb{R}_+$. Then we can approximate (41) by the quadrature

$$\bar{g}_N \ \coloneqq \ \sum_{i=1}^{N} w_i g(y_i) \qquad (42)$$

Then the error of this approximation is bounded by

$$|\ \bar{g} - \bar{g}_N\ | \le C_{quad}(\|g\|_{Z^*}, \bar{d})\ N^{-\alpha}\ ,\ \text{for some } \alpha > 0 \qquad (43)$$

These quadrature weights, quadrature points and α vary with $\bar{d}$'s range.

A.4.2 Applying Quadrature rule on Theorem 3.2

The loss function can then be written as

$$\begin{aligned}\mathcal{L}(\theta) \;=\; \mathcal{E}_T^2 \;:=\; & \frac{1}{N_{tb}} \underbrace{\sum_{n=1}^{N_{tb}} w_n^{tb} |\mathcal{R}_{tb,\theta^*}(x_n)|^2}_{(\mathcal{E}_T^{tb})^2} + \frac{1}{N_{sb}} \underbrace{\sum_{n=1}^{N_{sb}} w_n^{sb} |\mathcal{R}_{sb,-1,\theta^*}(t_{n,\delta})|^2}_{(\mathcal{E}_T^{sb,-1})^2} \\ & + \frac{1}{N_{sb}} \underbrace{\sum_{n=1}^{N_{sb}} w_n^{sb} |\mathcal{R}_{sb,1,\theta^*}(t_{n,\delta})|^2}_{(\mathcal{E}_T^{sb,1})^2} + \frac{\lambda}{N_{int}} \underbrace{\sum_{n=1}^{N_{int}} w_n^{int} |\mathcal{R}_{int,\theta^*}(x_n, t_{n,\delta})|^2}_{(\mathcal{E}_T^{int})^2} \end{aligned} \tag{44}$$

In our experiments we choose all w-s to be equal to 1 and train our model on that

Theorem A.2. *Let $u \in C^k((-1+\delta, \delta) \times (-1,1))$ be the unique solution of the viscous scalar conservation law for any $k \geq 1$. Let $u^* = u_{\theta^*}$ be the PINN, then the generalization error (10) is bounded by*

$$\begin{aligned}\mathcal{E}_G^2(u^*) \leq \left(1 + Ce^C\right) \Bigg[& \sum_{n=1}^{N_{tb}} w_n^{tb} |\mathcal{R}_{tb,\theta^*}(x_n)|^2 + \sum_{n=1}^{N_{int}} w_n^{int} |\mathcal{R}_{int,\theta^*}(x_n, t_{n,\delta})|^2 \\ & + 2C_{2b} \left(\sum_{n=1}^{N_{sb}} w_n^{sb} |\mathcal{R}_{sb,-1,\theta^*}(t_{n,\delta})|^2 + \sum_{n=1}^{N_{sb}} w_n^{sb} |\mathcal{R}_{sb,1,\theta^*}(t_{n,\delta})|^2 \right) + 2C_{1b} \left(\mathcal{E}_T^{sb,-1} + \mathcal{E}_T^{sb,1} \right) \\ & + \frac{C_{quad}^{tb}}{N_{tb}^{\alpha_{tb}}} + \frac{C_{quad}^{int}}{N_{int}^{\alpha_{int}}} + 2C_{2b} \left(\frac{\left(C_{quad}^{sb,-1} + C_{quad}^{sb,1}\right)}{N_{sb}^{\alpha_{sb}}} \right) + 2C_{1b} \left(\frac{\left(C_{quad}^{sb,-1} + C_{quad}^{sb,1}\right)}{N_{sb}^{\frac{\alpha_{sb}}{2}}} \right) \Bigg] \end{aligned} \tag{45}$$

where $C = 1 + 2C_{u_x}$, with

$$\begin{aligned} C_{u_x} &= \|u_x\|_{L^\infty} = \left\| \frac{1}{t-1} \right\|_{L^\infty([-1+\delta,\delta])} \\ C_{1b} &= \|u(1,t)\|_{L^\infty}^2 = \left\| \frac{1}{1-t} \right\|_{L^\infty([-1+\delta,\delta])}^2 \\ C_{2b} &= \|u_{\theta^*}(1,t)\|_{L^\infty([-1+\delta,\delta])} + \frac{3}{2} \left\| \frac{1}{t-1} \right\|_{L^\infty([-1+\delta,\delta])} \end{aligned} \tag{46}$$

and $C_{quad}^{tb} = C_{quad}^{tb}\left(\left\|\mathcal{R}_{tb,\theta^*}^2\right\|_{C_k}\right)$, $C_{quad}^{int} = C_{quad}^{int}\left(\left\|\mathcal{R}_{int,\theta^*}^2\right\|_C^{k-2}\right)$, $C_{quad}^{sb,-1} = C_{quad}^{sb,-1}\left(\|\mathcal{R}_{sb,-1,\theta^*}\|_{C^k}\right)$, $C_{quad}^{sb,1} = C_{quad}^{sb,1}\left(\left\|\mathcal{R}_{sb,1,\theta^*}^2\right\|_{C^k}\right)$ are constants of the quadrature bound.

Proof. In equation (40) within the proof of Theorem 3.2 we see that

$$\int_{-1+\delta}^{\delta} \int_{-1}^{1} \hat{u}^2(x,\bar{\delta}) dx d\bar{\delta} \leq C_T \int_{-1+\delta}^{\delta} \left[1 + \int_{-1+\delta}^{\bar{\delta}} Ce^C dt \right] d\bar{\delta}$$

$$\mathcal{E}_G^2 \leq \left[1 + Ce^C\right] C_T$$

where

$$\begin{aligned} C_T = & \underbrace{\int_{-1}^{1} \mathcal{R}_{tb,\theta^*}(x) dx}_{1} + \underbrace{2C_{2b} \left[\int_{-1+\delta}^{\delta} \mathcal{R}_{sb,-1,\theta^*}^2(t) dt + \int_{-1+\delta}^{\delta} \mathcal{R}_{sb,1,\theta^*}^2(t) dt \right]}_{3} \\ & + \underbrace{\int_{-1+\delta}^{\delta} \int_{-1}^{1} \mathcal{R}_{int,\theta^*}^2(x,t) dx dt}_{2} + \underbrace{2C_{1b} \left[\left(\int_{-1+\delta}^{\delta} \mathcal{R}_{sb,-1,\theta^*}^2 dt \right)^{\frac{1}{2}} + \left(\int_{-1+\delta}^{\delta} \mathcal{R}_{sb,1,\theta^*}^2 dt \right)^{\frac{1}{2}} \right]}_{4} \end{aligned} \tag{47}$$

Applying quadrature bounds on (47) we get,

$$
\begin{aligned}
C_T \leq & \underbrace{\sum_{n=1}^{N_{tb}} w_n^{tb} |\mathcal{R}_{tb,\theta^*}(x_n)|^2 + C_{quad}^{tb}(\|\mathcal{R}_{tb,\theta^*}\|_{C^k}) N_{tb}^{-\alpha_{tb}}}_{1} \\
& + \underbrace{\sum_{n=1}^{N_{int}} w_n^{int} |\mathcal{R}_{int,\theta^*}(x_n, t_{n,\delta})|^2 + C_{quad}^{int}(\|\mathcal{R}_{int,\theta^*}\|_{C^{k-2}}) N_{int}^{-\alpha_{int}}}_{2} \\
& + \underbrace{2C_{2b} \left[\sum_{n=1}^{N_{sb}} w_n^{sb} |\mathcal{R}_{sb,-1,\theta^*}(t_{n,\delta})|^2 + \sum_{n=1}^{N_{sb}} w_n^{sb} |\mathcal{R}_{sb,1,\theta^*}(t_{n,\delta})|^2 \right.}_{3} \\
& + \underbrace{\left. \left(C_{quad}^{sb}(\|\mathcal{R}_{sb,-1,\theta^*}\|_{C^k}) + C_{quad}^{sb}(\|\mathcal{R}_{sb,1,\theta^*}\|_{C^k}) \right) N_{sb}^{\alpha_{sb}} \right]}_{3} \\
& + \underbrace{2C_{1b} \left[\left(\sum_{n=1}^{N_{sb}} w_n^{sb} |\mathcal{R}_{sb,-1,\theta^*}(t_{n,\delta})|^2 \right)^{\frac{1}{2}} + \left(\sum_{n=1}^{N_{sb}} w_n^{sb} |\mathcal{R}_{sb,1,\theta^*}(t_{n,\delta})|^2 \right)^{\frac{1}{2}} \right.}_{4} \\
& + \underbrace{\left. \left(C_{quad}^{sb}(\|\mathcal{R}_{sb,-1,\theta^*}\|_{C^k}) + C_{quad}^{sb}(\|\mathcal{R}_{sb,1,\theta^*}\|_{C^k}) \right)^{\frac{1}{2}} N_{sb}^{\frac{\alpha_{sb}}{2}} \right]}_{4} \qquad (48)
\end{aligned}
$$

Replacing the sums of residuals by training error we get

$$
\begin{aligned}
\mathcal{E}_G^2 \leq & \left(1 + Ce^C\right) \left[\left(\mathcal{E}_T^{tb}\right)^2 + \left(\mathcal{E}_T^{int}\right)^2 + 2C_{2b} \left(\left(\mathcal{E}_T^{sb,-1}\right)^2 + \left(\mathcal{E}_T^{sb,1}\right)^2 \right) + 2C_{1b} \left(\mathcal{E}_T^{sb,-1} + \mathcal{E}_T^{sb,1} \right) \right] \\
& + \left(1 + Ce^C\right) \left[C_{quad}^{tb} N_{tb}^{-\alpha_{tb}} + C_{quad}^{int} N_{int}^{-\alpha_{int}} + 2C_{2b} \left(\left(C_{quad}^{sb,-1} + C_{quad}^{sb,1} \right) N_{sb}^{-\alpha_{sb}} \right) \right. \\
& \left. + 2C_{1b} \left(\left(C_{quad}^{sb,-1} + C_{quad}^{sb,1} \right) N_{sb}^{\frac{-\alpha_{sb}}{2}} \right) \right] \qquad (49)
\end{aligned}
$$

□

B PLOTTING THE BEHAVIOUR OF RHS OF EQUATION 11 WITH VARYING WIDTH

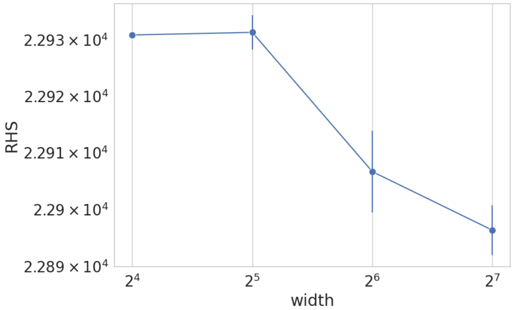

Figure 3: This plot tracks the RHS of equation (11) in Theorem 3.2 for training a depth 2 net at different widths towards solving equation 6 at $\delta = \frac{1}{2}$

C PLOTTING THE NEURALLY DERIVED SOLUTION FOR EQUATION 6 (LEFT) AND THE TRUE SOLUTION (RIGHT)

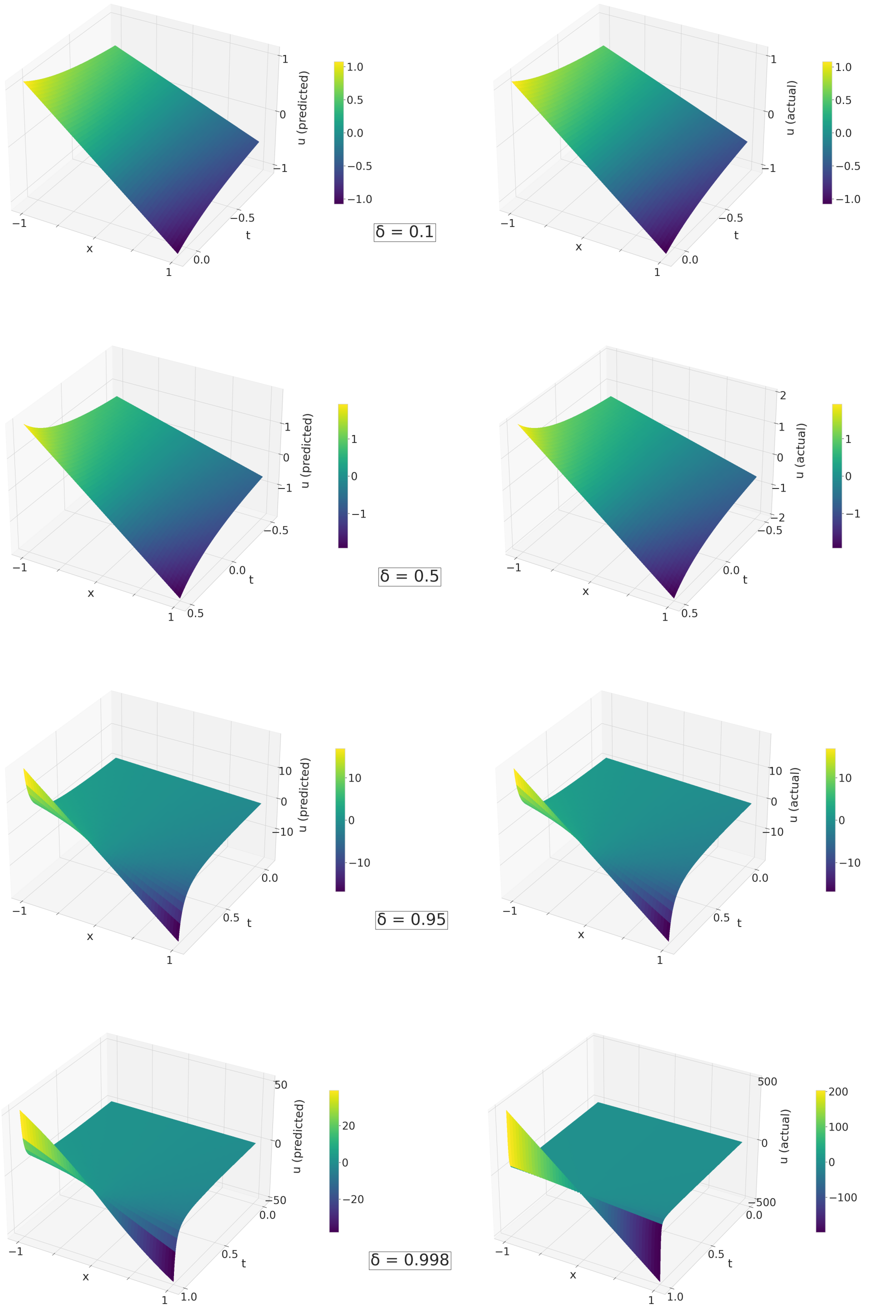

Figure 4: A demonstration of the visual resemblance between the neurally derived solution for equation 6 (left) and the true solution (right) at different values of the δ parameter getting close to the PDE with blow-up at $\delta = 1$. A PINN with a width of 300 and a depth of 6 was trained to generate the plots on the left.

D A STUDY OF THE APPROXIMATE INVARIANCE OF THE TRAINING TIME FOR THE 1D BURGERS' PDE VS PROXIMITY TO SINGULARITY

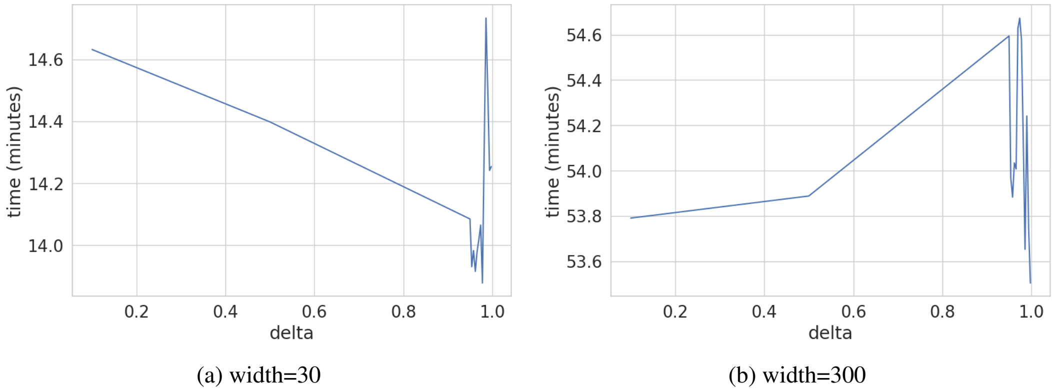

(a) width=30

(b) width=300

Figure 5: These plots show that the time taken to train a PINN on equation 6 barely changes for different values of δ - a measure of proximity to blow-up and that this holds at two widely separated widths of the net.

E INAPPLICABILITY OF CLASSICAL NUMERICAL ANALYSIS ERROR BOUNDS TO PINN EXPERIMENTS

To the best of our knowledge existing results in numerical analysis cannot be deployed to understand PINN training - as is the target here. Specifically for the 0 viscosity Burgers' PDE one can see that in works like Johnson & Szepessy (1987), the theory does not seem to be give a bound on the distance from the true solution of the solution found by the finite element method.

More generally, in works such as Corollary 3.5 in Tadmor (1991) the authors consider a weak solution of the ε-viscosity regularized Burgers' PDE and derive bounds on the local L^p-distance between the weak solution and the true solution at zero viscosity. There is no obvious way to apply these bounds for a PINN solution since the trained net has no guarantee to be satisfying the conditions required of the surrogate here.

For results like Theorem 2.1 in Nessyahu & Tadmor (1992), we observe that these too don't have an obvious way for the bounds to be applied for PINN experiments because they need stringent conditions (like satisfying the conservativeness property) to be true for the approximant, for the bounds to apply and there is no natural way to know if the neural surrogate satisfies these conditions. Also both the above cited classical bounds are not tailored to any compact domain and hence there is no boundary condition error that is getting tracked there as in our Theorem 3.2.